

The Significance of Fluctuating Charges for Molecular Polarizability and Dispersion Coefficients

YingXing Cheng¹ and Toon Verstraelen^{1, a)}

*Center for Molecular Modeling (CMM), Ghent University,
Technologiepark-Zwijnaarde 46, B-9052, Ghent, Belgium*

(Dated: 10 August 2023)

The influence of fluctuating charges or charge flow on the dynamic linear response properties of isolated molecules from the TS42 database is evaluated, with particular emphasis on dipole polarizability and C_6 dispersion coefficients. Two new descriptors are defined to quantify the charge-flow contribution to response properties, making use of the recoupled dipole polarizability to separate isotropic and anisotropic components. Molecular polarizabilities are calculated using the “frequency-dependent atom-condensed Kohn-Sham density functional theory approximated to second order”, i.e. the ACKS2 ω model. With ACKS2 ω , the charge-flow contribution can be constructed in two conceptually distinct ways, which appear to yield compatible results. The charge-flow contribution is significantly affected by molecular geometry and the presence of polarizable bonds, in line with previous studies. We show that the charge-flow contribution qualitatively reproduces the polarizability anisotropy. The contribution to the anisotropic C_6 coefficients is less pronounced, but cannot be neglected. The effect of fluctuating charges is only negligible for small molecules with at most one non-hydrogen atom. They become important and sometimes dominant for larger molecules or when highly polarizable bonds are present, such as conjugated, double or triple bonds. Charge flow contributions cannot be explained in terms of individual atomic properties, because they are affected by non-local features such as chemical bonding and geometry. Therefore, polarizable force fields and dispersion models can benefit from the explicit modeling of charge flow.

^{a)}Electronic mail: toon.verstraelen@ugent.be

I. INTRODUCTION

Van der Waals (vdW) dispersion interactions are ubiquitous non-bonded forces in molecular systems and materials, playing a crucial role in various applications in chemistry and physics. These interactions are relatively weak compared to bonded forces, yet universally attractive between all atoms due to the coupled motion of electrons at different sites. While classical models for the coupled electronic vibrations exist, only the zero-point oscillations in quantum-mechanical models can explain the persistence of vdW interactions at 0 K.¹ Density functional theory (DFT) is extensively employed in chemistry and physics, particularly for large systems, as it provides a favorable balance between computational accuracy and efficiency compared to more accurate wavefunction methods such as configuration interaction (CI) and coupled cluster (CC). However, one of the main challenges with DFT is its struggle to accurately describe the attractive part of vdW dispersion interactions, also known as long-range correlation energy, necessitating the development of appropriate dispersion corrections.

To address the lack of long-range correlation energy in DFT approximations, several correction terms have been proposed. Prominent correction schemes can be classified into three categories:² (i) semiclassical schemes, which apply corrections mainly to the total energy E , (ii) nonlocal, density-based functionals, which incorporate corrections to the electronic potential V , and (iii) one-electron effective potential methods, which rely on a single electron's potential for corrections. This study focuses on the first category, semiclassical schemes, as methods in this group explicitly use C_6 or higher-order dispersion coefficients, which play a significant role in determining the interaction strengths in molecular systems and materials. For more details about methods in other categories, refer to a recent review.³ Additionally, dispersion energy calculations have been extensively covered in numerous review articles.^{2,4-9}

The first quantum-mechanical dispersion model, by London, applied perturbation theory to the Coulomb interaction between electrons of two polarizable hydrogenic atoms.¹⁰ Building on London's work, the generalized Casimir-Polder (GCP) expression describes dispersion interactions for any pair of molecules A and B .¹¹ At long distances R , the leading attractive terms are proportional to R^{-6} , R^{-8} , R^{-10} , etc. Molecules are typically treated with a distributed multipole expansion, i.e. they are decomposed into sites, $a \in A$ and $b \in B$, treating each atom or group as a multipole polarizable site. Ignoring intra-molecular coupling

and non-local effects, the total dispersion energy is approximated by a simple pairwise-additive form.

$$E = - \sum_{ab} \sum_{n=6,8,10,\dots} f_n(R_{ab}) \frac{C_n^{ab}}{R_{ab}^n} \quad (1)$$

where R_{ab} is the distance between atoms a and b , and $f_n(R_{ab})$ is a damping function accounting for short-range phenomena. C_n^{ab} are dispersion coefficients, which can be expressed in terms of the frequency-dependent multipole polarizabilities of sites a and b . As the leading term in Eq. (1), the C_6 dispersion coefficients play a crucial role in determining the strengths of the dispersion interactions in molecular systems and materials. The conventional power laws are employed in most molecular force fields and empirical dispersion corrections for DFT.^{12–14}

The basic pairwise-additive form in Eq. (1) is only an approximation of the complete dispersion interaction between molecules A and B. The errors made by Eq. (1) were classified as different types of non-additivity.¹⁵ Type-A non-additivity arises when atomic C_n coefficients in a molecule deviate from those of isolated atoms.¹⁶ Type-B non-additivity emerges when the presence of a third atom or molecule screens the electrostatic interaction, modifying the dispersion interaction compared to just having molecules A and B in vacuum. Recent studies have suggested that Type-B non-additivity can also be interpreted as a manifestation of electric many-body effects.¹⁷ Type-C non-additivity is observed in low-dimensional nanostructures or metallic systems, where long-range charge fluctuations result in dispersion interactions with non-standard power laws, with a smaller magnitude of the exponent of R .¹⁸

Semiclassical models with pairwise expressions, such as Eq. (1), including Grimme's DFT+D n ($n = 1, 2, 3, 4$) schemes,^{19–23} Tkatchenko and Scheffler (TS) method,¹³ the exchange-hole dipole moment (XDM) method by Becke and Johnson,^{12,24,25} and the local-response dispersion (LRD) model by Sato and Nakai,^{26–28} consider type-A non-additive dispersion interactions.¹⁵ However, only a few models partially account for type-B non-additivity, as simple pairwise methods struggle with many-body effects. DFT+D3 and DFT+D4 methods include the three-body Axilrod-Teller-Muto (ATM) term,^{29,30} and XDM can describe type-B interactions through electronic many-body effects.^{17,31} Although the atomic three-body ATM term can be added in XDM, its contribution is typically small compared to higher-order two-body dispersion terms, suggesting that atomic many-body effects might be negligible.^{32,33} A well-known method for fully treating both type-A and type-B

non-additive dispersion energy is the many-body dispersion model (MBD),^{34–36} based on dipolar coupling between atomic quantum harmonic oscillators. In addition, MBD also exhibits significant deviations from common power laws, which is normally associated with charge flow in type-C dispersion.³⁷ However, all models mentioned so far treat atoms as local (dipole and optionally higher multipole) polarizable sites, neglecting fluctuating charges or monopoles, which are the leading term of distributed multipole expansion.

Fluctuating charges can contribute significantly to the dispersion energy,³⁸ and they become essential in systems where the GCP equation is insufficient. For example, dispersion interactions are critically affected by monopolar effects in carbon nanomaterials,^{7,39,40} traditional semiconductors,^{41,42} and low-dimensional materials.^{39,43} In the presence of delocalized bonds, monopolar fluctuations exhibit complex non-local features related to resonance.⁴⁴ Charge fluctuations have been used to model specific dispersion interactions, e.g., between infinite wires and slabs,^{39,45,46} and in fullerenes and aromatic systems.^{47,48} A recent study by Dobson shows that local models, e.g., MBD, cannot capture type-C non-additive dispersion interactions, which are related to long-range charge fluctuations.⁴⁰ To further explore the relevance of charge fluctuations, this work focuses on their impact on the polarizability and dispersion interaction of a more general set of molecules or molecular dimers. Understanding the contribution of fluctuating charges to polarizability and C_6 dispersion coefficients is crucial for developing more accurate polarizable force fields and dispersion models that can better describe the behavior of molecular systems and materials.

Previous studies have examined the significant contributions of charge-flow effects on static dipole polarizabilities in various systems, such as silicon clusters,^{41,42} water and water-ion clusters,^{49,50} hydrated methane sulfonic acid (MSA) clusters,⁵¹ and stoichiometric aluminum phosphide clusters.⁵² Recent work has also revealed that these effects can strongly influence the polarizability anisotropy, with the specific partitioning scheme employed further influencing the magnitude of their contribution.⁵³ Anisotropic polarization naturally leads to dispersion anisotropy, which was recently identified as a driving force for the conformational stability of macromolecules.⁵⁴ However, the influence of charge fluctuations on the anisotropy of frequency-dependent polarizabilities and dispersion coefficients has not been fully explored. This paper aims to address this knowledge gap by investigating the impact of charge fluctuations on the anisotropy of frequency-dependent dipole polarizabilities and

C_6 dispersion coefficients in a more general set of molecules or molecular dimers.

To accurately investigate the contribution of charge flow to linear-response properties, non-local distributed polarizabilities must be computed. These polarizabilities can be determined using various methods, broadly categorized into two groups. The first group involves numerical partitioning of molecular properties in Hilbert space, such as distributed multipole analysis (DMA),⁵⁵ LoProp,^{56,57} MoProp,⁵⁸ QUAMBO,⁵⁹ IAO/QUAO,^{60–62} as well as methods based on constrained density fitting.⁶³ While successful in developing useful models for polarization energies and dispersion models, these methods go beyond the scope of the current work. The second category of methods operate in real space, by defining distributed multipole operators as products of an atom-in-molecule (AIM) weight functions and regular multipole operators. The AIM weight functions determine the proportion of molecular density attributed to each atom, using partitioning schemes such as QTAIM,^{64,65} (Iterative) Hirshfeld,^{66,67} Iterative Stockholder,^{68,69} and so on. AIM weight functions directly partition the electron density, which also makes them trivially applicable to partitioning of density response kernels. In any case, all methods in the two categories can be employed to derive distributed polarizabilities from the interacting linear-response kernel, which can be computationally demanding for large-scale systems.

In this paper, we present an alternative approach to studying the impact of charge flow effects on the frequency-dependent linear-response properties of molecules. Specifically, we utilize a novel polarizable force field called “frequency-dependent atom-condensed Kohn-Sham density functional theory approximated to second order” (ACKS2 ω), which was introduced in previous works.^{70–72} This approach partitions both the hardness and non-interacting response kernels and can reproduce response properties with high accuracy. It even captures correct trends with fluctuating charges alone. We employ ACKS2 ω to compute the frequency-dependent response properties, including isotropic and anisotropic dipole polarizabilities and C_6 dispersion coefficients, of all molecules in the TS42 database, which is a diverse selection of organic and inorganic molecules.¹³ We then investigate the significance of charge-flow using two descriptors, for isotropic and anisotropic response properties, respectively. Our methodology yields valuable insights into the dominant contributors to the molecular polarizability and C_6 coefficients, shedding light on the role of fluctuating atomic charges in the dynamic linear-response properties of finite systems. Our results can inform

the development of more accurate polarizable force fields and dispersion models in the future.

For the definition of response basis functions in the ACKS2 ω model, an atoms-in-molecules method is used, analogous to our previous publications.^{71,72} Practically, multiple definitions of atoms in molecules exist, each having specific advantages, e.g., in terms of interpretability and robustness. We employ one of these methods in this work, namely Minimal Basis Iterative Stockholder,⁷³ and slightly different results may be obtained when using another AIM scheme. Still, we believe the general trends to hold across different AIM definitions, as they did in previous works.⁵³

The remainder of this paper is structured as follows. In Section II, we describe the relevant methodology for this study. We begin by defining charge-flow distributed polarizabilities and then introduce the concept of recoupled dipole polarizability, which we use to define the anisotropy of the (frequency-dependent) dipole polarizability. Moreover, we show that anisotropic C_6 coefficients can also be defined using the recoupled dipole polarizability. Furthermore, we introduce two descriptors to compute the ratio of charge-flow contribution to various linear-response properties. In Section III, we provide computational details on the ACKS2 ω model, the reference TD-DFT calculations, and introduce notation to describe the charge-flow and other contributions. The results and discussion are presented in Sections IV and V, respectively. Lastly, a summary is given in Section VI. Atomic units are used throughout.

II. METHODS

In this section, we introduce the theory used in this work. First, we describe charge-flow distributed polarizabilities, as defined in Ref. 74. Next, we introduce recoupled dipole polarizabilities to define the anisotropy of dipole polarizability and C_6 dispersion coefficients. Finally, we introduce two descriptors to study the charge-flow contribution to dipole polarizability and C_6 coefficients.

A. Charge-flow contribution to the polarizability

The response of a molecule's charge density $\Delta\rho(\mathbf{r}',\omega)$ to an external field $V(\mathbf{r},\omega)$ at position \mathbf{r} can be described by the density response function $\chi(\mathbf{r},\mathbf{r}',\omega)$, which quantifies the

change in charge density at position \mathbf{r}' . This relationship can be expressed by the following equation:

$$\Delta\rho(\mathbf{r}', \omega) = - \int d\mathbf{r} V(\mathbf{r}, \omega) \chi(\mathbf{r}, \mathbf{r}', \omega). \quad (2)$$

One way to represent an external potential is through real spherical harmonics $R_{\ell\kappa}(\mathbf{r})$ and their corresponding fields $V_{\ell\kappa}(\omega)$ as $\sum_{\ell\kappa} R_{\ell\kappa}(\mathbf{r}) V_{\ell\kappa}(\omega)$, following Stone's notation.³⁸ With this representation, the change in charge density can be expressed as:

$$\Delta\rho(\mathbf{r}', \omega) = - \int \chi(\mathbf{r}, \mathbf{r}', \omega) \sum_{\ell\kappa} R_{\ell\kappa}(\mathbf{r}) V_{\ell\kappa}(\omega) d\mathbf{r}, \quad (3)$$

and the response multipole moments related to $R_{\ell'\kappa'}(\mathbf{r}')$ are

$$\Delta\mu_{\ell'\kappa'}(\omega) = \int d\mathbf{r}' \Delta\rho(\mathbf{r}', \omega) R_{\ell'\kappa'}(\mathbf{r}') \quad (4)$$

As a result, the spherical-tensor polarizability $\alpha_{\ell\kappa, \ell'\kappa'}(\omega)$ can be determined through the following equation:

$$\alpha_{\ell\kappa, \ell'\kappa'}(\omega) = \int R_{\ell\kappa}(\mathbf{r}) \chi(\mathbf{r}, \mathbf{r}', \omega) R_{\ell'\kappa'}(\mathbf{r}') d\mathbf{r} d\mathbf{r}'. \quad (5)$$

The molecular dipole polarizability, represented as a 3×3 matrix, can be obtained with $\ell = \ell' = 1$.

The radius of convergence of the single-site molecular polarizability is limited by the largest distance between the molecular center and a point inside the molecule.⁷⁴ To overcome this limitation, distributed polarizabilities have been proposed, where a molecule is divided into atomic regions, and the potential is expanded using multipoles or Taylor series about each local center. The external potential can then be expressed as a sum of the potentials of the regions. The spherical-tensor form, similar to Eq. (5), is used, and the external potential can be written as:

$$V(\mathbf{r}, \omega) = \sum_a w_a(\mathbf{r}) \sum_{\ell\kappa} R_{\ell\kappa}(\mathbf{r} - \mathbf{R}^a) V_{\ell\kappa}^a(\omega), \quad (6)$$

where $w_a(\mathbf{r})$ is the AIM weight function ($0 \leq w_a(\mathbf{r}) \leq 1$) that determines which portion of the total electron density is attributed to atom a . Within each atom a , a standard multipole expansion is used with fields $V_{\ell\kappa}^a(\omega)$ and spherical harmonics $R_{\ell\kappa}$, which use \mathbf{R}^a , the nucleus of atom a , as origin.³⁸

The distributed polarizability is defined by the following expression:⁷⁵

$$\alpha_{\ell\kappa,\ell'\kappa'}^{aa'}(\omega) = \iint d\mathbf{r}d\mathbf{r}' Q_{\ell\kappa,\ell'\kappa'}^a(\mathbf{r})\chi(\mathbf{r},\mathbf{r}',\omega)Q_{\ell'\kappa'}^b(\mathbf{r}') \quad (7)$$

where $Q_{\ell\kappa}^a(\mathbf{r}) = w_a(\mathbf{r})R_{\ell\kappa}(\mathbf{r} - \mathbf{R}^a)$ is the distributed multipole moment with rank $\ell\kappa$ of atom a .

For a homogeneous electric field along the x -axis, the multipole expansion is given by

$$x = \sum_a w_a(\mathbf{r})X^a + \sum_a w_a(\mathbf{r})(x - X^a) \quad (8)$$

where X^a is the x -component of atomic coordinate \mathbf{R}^a . With this decomposition of a homogeneous field, distributed contributions to the dipole polarizability can be defined, for which a more convenient notation than that of Eq. (7) can be used. The frequency-dependent charge-flow, charge-dipole, and dipole-only distributed polarizabilities are defined, respectively, as

$$\alpha_{00}^{ab}(\omega) = \int d\mathbf{r}d\mathbf{r}' w_a(\mathbf{r})\chi(\mathbf{r},\mathbf{r}',\omega)w_b(\mathbf{r}') \quad (9)$$

$$\alpha_{0j}^{ab}(\omega) = \int d\mathbf{r}d\mathbf{r}' w_a(\mathbf{r})\chi(\mathbf{r},\mathbf{r}',\omega)w_b(\mathbf{r}')(\mathbf{r}_j - \mathbf{R}_j^b) \quad (10)$$

$$\alpha_{ij}^{ab}(\omega) = \int d\mathbf{r}d\mathbf{r}' w_a(\mathbf{r})(\mathbf{r}_i - \mathbf{R}_i^a)\chi(\mathbf{r},\mathbf{r}',\omega)w_b(\mathbf{r}')(\mathbf{r}_j - \mathbf{R}_j^b), \quad (11)$$

where i or j represents x , y or z . The total molecular polarizability $\alpha_{ij}(\omega)$ is reconstructed from these contributions with:³⁸

$$\alpha_{ij}(\omega) = \sum_{ab} (\mathbf{R}_i^a \mathbf{R}_j^b \alpha_{00}^{ab}(\omega) + \mathbf{R}_i^a \alpha_{0j}^{ab}(\omega) + \mathbf{R}_j^b \alpha_{i0}^{ab}(\omega) + \alpha_{ij}^{ab}(\omega)), \quad (12)$$

In this study, we investigate the charge-flow contribution to the distributed polarizability of molecules, specifically the α_{00}^{ab} term. We define the charge-flow (CF) contribution to the molecular dipole polarizability as follows:^{49–52,76–79}

$$\alpha_{ij}^{\text{CF}} = \sum_{ab} \mathbf{R}_i^a \mathbf{R}_j^b \alpha_{00}^{ab} \quad (13)$$

This definition differs from that used in previous work by Jackson and co-workers^{41,42,53}, where the CF contribution is defined as:

$$\alpha_{ij}^{\text{CF}} = \sum_a R_i^a \int w_a(\mathbf{r})\Delta\rho_j(\mathbf{r})d\mathbf{r} = \sum_{ab} (\mathbf{R}_i^a \mathbf{R}_j^b \alpha_{00}^{ab} + \mathbf{R}_i^a \alpha_{0j}^{ab}) \quad (14)$$

In the above equation, $\Delta\rho_j(\mathbf{r})$ is the response density resulting from a homogeneous electric field applied along the j axis. Our focus, however, is solely on the charge-flow contribution described by Eq. (13).

B. Recoupled dipole polarizability

The definition of dipole polarizability in Eq. (5) uses two spherical harmonics, which can be expressed more elegantly using single harmonics, as has been extensively covered in previous studies.^{38,80} We provide a brief summary of this concept here for the sake of clarity, and the frequency is omitted in this subsection for simplicity.

The components α_{LK} of the recoupled dipole polarizability are defined as

$$\begin{bmatrix} \alpha_{00} \\ \alpha_{20} \\ \alpha_{21c} \\ \alpha_{21s} \\ \alpha_{22c} \\ \alpha_{22s} \end{bmatrix} = \sqrt{\frac{2}{3}} \begin{bmatrix} -\frac{\sqrt{2}}{2} & 0 & 0 & -\frac{\sqrt{2}}{2} & 0 & -\frac{\sqrt{2}}{2} \\ -\frac{1}{2} & 0 & 0 & -\frac{1}{2} & 0 & 1 \\ 0 & 0 & \sqrt{3} & 0 & 0 & 0 \\ 0 & 0 & 0 & 0 & \sqrt{3} & 0 \\ \frac{\sqrt{3}}{2} & 0 & 0 & -\frac{\sqrt{3}}{2} & 0 & 0 \\ 0 & \sqrt{3} & 0 & 0 & 0 & 0 \end{bmatrix} \begin{bmatrix} \alpha_{xx} \\ \alpha_{xy} \\ \alpha_{xz} \\ \alpha_{yy} \\ \alpha_{yz} \\ \alpha_{zz} \end{bmatrix} \quad (15)$$

where L can be either 0 or 2 and K can be 0, 1c, 1s, 2c, or 2s. (See Ref. 38 for more details.)

The isotropic dipole polarizability, denoted as α^{iso} or $\bar{\alpha}$, can be expressed in terms of the component α_{00} as:

$$\alpha^{\text{iso}} = \frac{1}{3}(\alpha_{xx} + \alpha_{yy} + \alpha_{zz}) = -\sqrt{\frac{1}{3}}\alpha_{00} \quad (16)$$

The anisotropic dipole polarizability, denoted as $\vec{\alpha}$, is a vector composed of all elements α_{LK} with $L = 2$. It can be written as:

$$\vec{\alpha} = \sqrt{\frac{1}{3}}(\alpha_{20}, \alpha_{21c}, \alpha_{21s}, \alpha_{22c}, \alpha_{22s}), \quad (17)$$

where $\sqrt{\frac{1}{3}}$ is a new prefactor instead of $\sqrt{\frac{3}{2}}$ in Ref. 38, in order to maintain consistency with the definition of isotropic dipole polarizability using recoupled polarizability. The anisotropy of the dipole polarizability, denoted as $\|\vec{\alpha}\|$, is defined as:³⁸

$$\begin{aligned} \|\vec{\alpha}\|^2 &= \frac{1}{3} \sum_q |\alpha_{2q}|^2 \\ &= \frac{2}{3}(\alpha_{xy}^2 + \alpha_{xz}^2 + \alpha_{yz}^2) + \frac{1}{9}[(\alpha_{xx} - \alpha_{yy})^2 + (\alpha_{xx} - \alpha_{zz})^2 + (\alpha_{yy} - \alpha_{zz})^2], \end{aligned} \quad (18)$$

where the summation is taken over all K values associated with $L = 2$ in Eq. (15). It should be noted that anisotropy can be defined in terms of the tensor eigenvalues, which has the

TABLE I. The factor $N(L_A, L_B, J)$.

L_A	L_B	J	$N(L_A, L_B, J)$
0	0	0	$1/\pi$
0	2	2	$-\sqrt{2}/2\pi$
2	0	2	$-\sqrt{2}/2\pi$
2	2	0	$1/10\pi$
2	2	2	$1/7\pi$
2	2	4	$54/35\pi$

same form as Eq. (18) without the off-diagonal elements.^{53,81,82} However, both definitions are equivalent, and Eq. (18) can be systematically extended to define the anisotropy of higher-multipole polarizabilities. Thus, we use Eq. (18) as the definition of anisotropy in this work.

C. C_6 dispersion coefficients

The C_6 dispersion coefficients of a pair of molecules are expressed in terms of the frequency-dependent polarizabilities of the individual molecules, as shown in Ref. 80:

$$C_6(L_A L_B J; K_A K_B) = N(L_A, L_B, J) \int_0^\infty \alpha_{L_A K_A}^A(i\nu) \alpha_{L_B K_B}^B(i\nu) d\nu, \quad (19)$$

where $|L_A - L_B| \leq J \leq L_A + L_B$, and A and B refer to the molecules. According to previous work,^{38,80,83} C_6 with odd J is negligible, so we only consider C_6 with even J . The prefactor N depends on L_A , L_B , and J , and its values are shown in Table I.

The isotropic C_6 coefficient, denoted as C_6^{iso} , can be expressed as $C_6(000; 00)$:

$$C_6^{\text{iso}} = C_6(000; 00) = \frac{3}{\pi} \int_0^\infty \bar{\alpha}^A(i\nu) \bar{\alpha}^B(i\nu) d\nu. \quad (20)$$

In analogy to the dipole polarizability in Section II B, the anisotropic C_6 coefficients are collected in a vector \vec{C}_6 , which comprises all elements $C_6(L_A L_B J; L_A L_B)$ that satisfy the condition $L_A + L_B + J \neq 0$. When $L_A = 0$ ($L_B = 0$), the K_A (K_B) is restricted to 0, whereas for $L_A = 2$ ($L_B = 2$), the possible values for K_A (K_B) include “00”, “20”, “21c”, “21s”, “22c”, and “22s”. Consequently, \vec{C}_6 encompasses 85 distinct components. The anisotropy of C_6 ,

denoted as $\|\vec{C}_6\|$, is defined analogously to $\|\vec{\alpha}\|$:

$$\|\vec{C}_6\|^2 = \sum_{L_A+L_B+J \neq 0} |C_6(L_A L_B J; K_A K_B)|^2. \quad (21)$$

Using the definition in Eq. (19), the long-range dispersion energy, which accounts for molecular polarizability anisotropy, is given by:

$$E = - \sum_{n=6,8,10,\dots} \frac{1}{R_{AB}^n} \sum_{L_A, L_B, J} \sum_{K_A, K_B} C_n^{AB}(L_A L_B J; K_A K_B) \bar{S}_{L_A L_B J}^{K_A K_B} \quad (22)$$

where $\bar{S}_{L_A L_B J}^{K_A K_B}$ depends on the relative orientation between molecules A and B .⁸⁰

D. Descriptors to quantify different contributions to polarizability and dispersion

In this study, the dipole polarizability or the dispersion coefficients will be computed with different forms of the ACKS2 model. As explained in the following section, ACKS2 allows us to isolate specific contributions, such as charge flow, to these quantities. The importance of a contribution, for any given molecule, will be quantified with descriptors defined below. For the definition of these descriptors, generic symbols X^{iso} , \vec{X} and $\|\vec{X}\|^2$ are used below, where X could refer to polarizability or dispersion coefficients, presented in sections II B and II C, respectively. The subscript c is added to denote a contribution of interest: X_c^{iso} , \vec{X}_c and $\|\vec{X}_c\|^2$. The absence of a subscript in X , or the subscript “ref”, will be used to refer to the reference result computed directly with TD-DFT. Plots and statistical properties of the descriptors will be used to summarize the detailed results for the entire TS42 database.¹³ The relevant dimensionless descriptors are defined as follows:

- The descriptor s quantifies the isotropic part of contribution c relative to its reference value:

$$s_c[X] = \frac{X_c^{\text{iso}}}{X^{\text{iso}}} \quad (23)$$

Because the isotropic property in the denominator of $s_c[X]$ is always non-zero in practice, this ratio is well-defined.

- The fractional anisotropy of a property X , which is independent of the contribution being considered:

$$u[X] = \frac{\|\vec{X}\|^2}{\|\vec{X}\|^2 + (X^{\text{iso}})^2} \quad (24)$$

For symmetric molecules, $u[X]$ may become zero. This descriptor will be analyzed as such to illustrate the overall anisotropy of the molecular properties under study.

- The scalar product of \vec{X} and a contribution c to \vec{X} , normalized in the same way as $u[X]$:

$$u_c^{\parallel}[X] = \frac{\vec{X} \cdot \vec{X}_c}{\|\vec{X}\|^2 + (X^{\text{iso}})^2} \quad (25)$$

The term $(X^{\text{iso}})^2$ is included in the denominator to avoid divisions by zero for molecules lacking anisotropy. The symbol \parallel indicates that this descriptor only considers the contribution of vector \vec{X}_c along the vector \vec{X} . This descriptor is ideally close to $u[X]$.

Because $u[X]$ may become zero for symmetric molecules, the descriptor $u_c^{\parallel}[X]$ cannot be safely normalized on $u[X]$. Moreover, $u[X]$ can be interpreted as $u_c^{\parallel}[X]$ when $\vec{X}_c = \vec{X}$. The notation $u_{\text{ref}}^{\parallel}[X]$ is used to represent $u[X]$ in the remainder of the text, to emphasize that it is the reference value that includes all contributions.

Note that the descriptor $u[X]$ is guaranteed to lie in the interval $[0, 1]$. The two other descriptors, $s_c[X]$ and $u_c^{\parallel}[X]$, can be interpreted on the same scale, but are not guaranteed to remain within the $[0, 1]$ interval, of which some examples can be found in the results.

III. COMPUTATIONAL DETAILS

In this study, we investigated the impact of charge flow on dipole polarizabilities and C_6 coefficients, including their anisotropies, for all molecules in the TS42 database. The LDA/aug-cc-pVDZ level of theory^{84,85} was used for all response calculations, as it resulted in a good correspondence with experimental data in our previous work.⁷²

The frequency-dependent dipole polarizabilities were computed using the ACKS2 ω model with bi-orthogonal atomic potential and density basis sets, as described in Ref. 72: The potential basis set consists of distributed multipole operators defined with MBIS partitioning⁷³ and the density basis set is derived from a Fukui function and the non-interacting response

to the distributed multipole operators. To isolate the contribution of charge flow to the molecular dipole polarizability, ℓ_{\max} was set to 0 in the construction of the basis functions for ACKS2, which is denoted as contribution $c = 0$. The charge and dipole contributions to the molecular dipole polarizability were computed by setting $\ell_{\max} = 1$, which is denoted as contribution $c = 1$. Further exploration of $\ell_{\max} > 1$ is not expected to yield qualitatively different results because the ACKS2 model with $\ell_{\max} = 1$ already quantitatively reproduces frequency-dependent linear response, as will be shown in the results.⁷² We defined more fine-grained contributions to the $\ell_{\max} = 1$ result by considering the four terms in Eq. (12): the first is due to charge-flow, labeled $c = 1(0)$, the second and third terms are due to charge-dipole interactions, labeled $c = 1(1)$, and the last is due to dipole-only fluctuations, labeled $c = 1(2)$. One would not expect qualitative differences between $c = 0$ and $c = 1(0)$ *a priori* as they are two slightly different ways of modeling the charge-flow contribution to the polarizability.

The integral in Eq. (19) was evaluated using Gaussian-Legendre quadrature with 12 imaginary frequencies to calculate C_6 coefficients. The same frequencies were also used to study the relative charge-flow contribution to the frequency-dependent dipole polarizabilities. Because C_6 is calculated from two molecular dipole polarizabilities, the integer indices 0, 1 and 2 to classify multipole contributions in Eq. (12) appear twice, once for molecule A and once for molecule B, leading to six categories of contributions to the dispersion coefficients, labeled as 1(00), 1(01), 1(02), 1(11), 1(12), or 1(22). There is no distinction between e.g. 1(01) and 1(10), because all $N^2 = 1764$ molecular dimers were considered to collect the statistics, as opposed to only the unique $N(N+1)/2 = 903$ pairs in our previous work.⁷² Table II provides an overview of all possible contributions to the polarizability and the dispersion coefficients.

All calculations were performed using the Horton package,⁸⁶ using the methodology described in Ref. 72. Reference TD-DFT calculations were performed with Dalton 2020.⁸⁷

Figure 1 illustrates the computational workflow to obtain the above descriptors, for the case of the static dipole polarizability of carbon monoxide. The upper part (blue boxes) represents the processing of TD-DFT reference results: by recoupling of the Cartesian tensors, the isotropic and anisotropic components are separated, which are then used as input for the descriptors (green box). The lower part (yellow and orange boxes) show the ACKS2 ω branch, whose main difference is the additional decomposition of the dipole polarizability

TABLE II. Overview of all considered contributions c to the dipole polarizability and the dispersion coefficient. For the ACKS2 ω model with $\ell_{\max} = 1$, the contributions to the response are decomposed further by grouping terms in Eq. (12): charge-flow (first term), charge-dipole (second and third term), dipole-dipole (fourth term). For the dispersion coefficient, this classification of terms must be applied to both molecules A and B in the dimer. Symmetrically equivalent cases are combined into one contribution.

Quantity	Contribution c	Model	Molecule A	Molecule B
Polarizability α	ref	TD-DFT Reference		
	0	ACKS2 ω $\ell_{\max} = 0$	all	–
	1	$\ell_{\max} = 1$	all	–
	1(0)	$\ell_{\max} = 1$ charge-flow		–
	1(1)	$\ell_{\max} = 1$ charge-dipole		–
	1(2)	$\ell_{\max} = 1$ dipole-dipole		–
Dispersion C_6	ref	TD-DFT Reference		
	0	ACKS2 ω $\ell_{\max} = 0$	all	all
	1	$\ell_{\max} = 1$	all	all
	1(00)	$\ell_{\max} = 1$ charge-flow	charge-flow	charge-flow
	1(01)	$\ell_{\max} = 1$ charge-flow	charge-flow	charge-dipole
	1(02)	$\ell_{\max} = 1$ charge-flow	charge-flow	dipole-dipole
	1(11)	$\ell_{\max} = 1$ charge-dipole	charge-dipole	charge-dipole
	1(12)	$\ell_{\max} = 1$ charge-dipole	charge-dipole	dipole-dipole
	1(22)	$\ell_{\max} = 1$ dipole-dipole	dipole-dipole	dipole-dipole

to isolate of different contributions, here charge flow [CF, $c = 1(0)$]. Also the recoupled ACKS2 ω tensors are used as input for the descriptors (green box). A similar workflow is used for dispersion coefficients, for which frequency-dependent polarizabilities at multiple imaginary frequencies are combined.

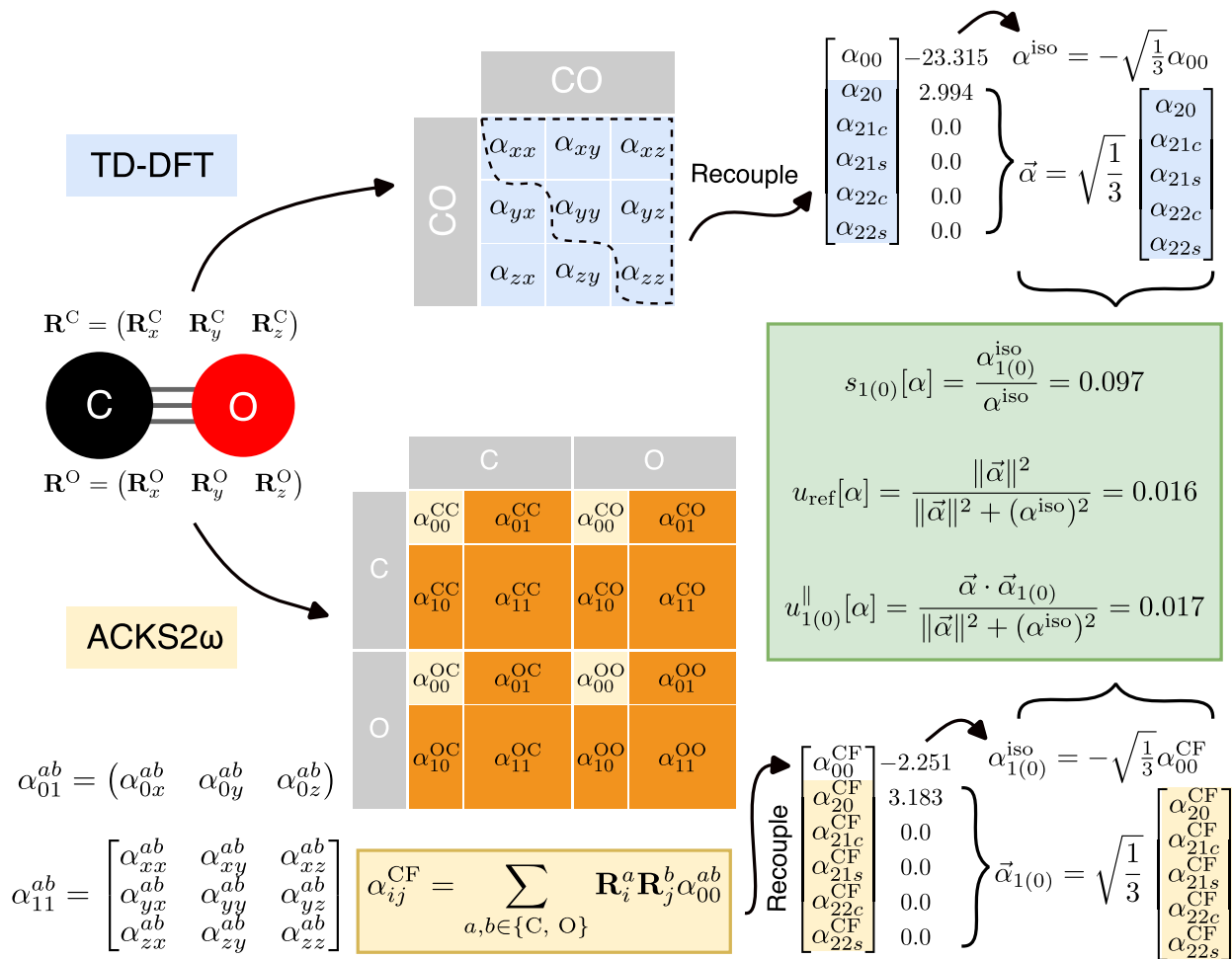


FIG. 1. The computational workflow to derive the polarizability descriptors from the TD-DFT and ACKS2 ω ($\ell_{max} = 1$) frequency-dependent polarizability tensors, for the case of carbon monoxide. See text for details.

IV. RESULTS

A. Isotropic dipole polarizability

Table III presents the values of $s_c[\alpha(0)]$, i.e. the static case, for various contributions c . Supplementary Tables S1-S12 show similar results at other imaginary frequencies. Figure 2 displays violin plots of $s_c[\alpha(0)]$ for different contributions c .

The charge-flow descriptors $s_0[\alpha(0)]$ (average 0.237) and $s_{1(0)}[\alpha(0)]$ (average 0.247) are very close. Except for slight differences, all results for $c = 0$ and $c = 1(0)$ are consistent, confirming that these are two comparable definitions of the charge-flow contribution. Any

This is the author's peer reviewed, accepted manuscript. However, the online version of record will be different from this version once it has been copyedited and typeset.
PLEASE CITE THIS ARTICLE AS DOI: 10.1063/5.0163842

TABLE III. Isotropic descriptors $s_c[\alpha(0)]$ for all molecules in the TS42 database, for each contribution c , as documented in Table II.

Molecule	$s_0[\alpha(0)]$	$s_1[\alpha(0)]$	$s_{1(0)}[\alpha(0)]$	$s_{1(1)}[\alpha(0)]$	$s_{1(2)}[\alpha(0)]$
C ₈ H ₁₈	0.417	0.988	0.429	0.218	0.341
C ₇ H ₁₆	0.404	0.988	0.415	0.224	0.349
C ₆ H ₆	0.404	0.965	0.414	0.204	0.348
C ₆ H ₁₄	0.387	0.987	0.398	0.230	0.359
C ₅ H ₁₂	0.365	0.986	0.377	0.238	0.372
CH ₃ CH ₂ OCH ₂ CH ₃	0.358	0.985	0.368	0.230	0.388
C ₄ H ₁₀ O	0.354	0.983	0.365	0.234	0.384
C ₄ H ₁₀	0.337	0.986	0.348	0.248	0.391
C ₄ H ₈	0.336	0.984	0.347	0.260	0.377
C ₃ H ₇ OH	0.322	0.982	0.332	0.242	0.408
CH ₃ CH ₃ CH ₃ N	0.318	0.981	0.329	0.244	0.408
CH ₃ COCH ₃	0.312	0.974	0.329	0.222	0.422
C ₃ H ₆	0.309	0.975	0.319	0.222	0.434
C ₃ H ₈	0.299	0.985	0.308	0.258	0.419
CCl ₄	0.299	0.905	0.303	0.126	0.475
CH ₃ OCH ₃	0.284	0.982	0.292	0.254	0.437
CH ₃ CHO	0.273	0.970	0.291	0.224	0.456
CH ₃ NHCH ₃	0.283	0.981	0.291	0.260	0.430
C ₂ H ₅ OH	0.278	0.980	0.286	0.248	0.447
CS ₂	0.267	0.899	0.276	0.140	0.484
N ₂ O	0.235	0.934	0.270	0.162	0.504
CO ₂	0.214	0.957	0.258	0.152	0.548
C ₂ H ₆	0.249	0.984	0.257	0.264	0.463
C ₂ H ₄	0.236	0.970	0.244	0.220	0.506
COS	0.218	0.922	0.242	0.128	0.552
SiH ₄	0.235	0.975	0.242	0.194	0.540
SO ₂	0.217	0.923	0.236	0.140	0.547
H ₂ CO	0.211	0.967	0.225	0.224	0.517
CH ₃ NH ₂	0.215	0.978	0.222	0.254	0.503
CH ₃ OH	0.212	0.978	0.219	0.248	0.510
C ₂ H ₂	0.183	0.966	0.190	0.176	0.600
Cl ₂	0.156	0.894	0.156	0.108	0.631
CH ₄	0.148	0.983	0.151	0.246	0.585
N ₂	0.104	0.941	0.114	0.148	0.681
CO	0.090	0.932	0.097	0.120	0.715
H ₂ S	0.083	0.932	0.086	0.130	0.716
NH ₃	0.078	0.972	0.080	0.190	0.703
H ₂ O	0.063	0.971	0.065	0.178	0.727
H ₂	0.061	0.993	0.062	0.184	0.748
HBr	0.051	0.930	0.053	0.074	0.803
HCl	0.046	0.926	0.047	0.078	0.801
HF	0.045	0.973	0.047	0.134	0.791
Min.	0.045	0.894	0.047	0.074	0.341
Max.	0.417	0.993	0.429	0.264	0.803
Mean	0.237	0.964	0.247	0.197	0.520

deviation between the two is due to the difference in ACSK2 basis set for $\ell_{\max} = 0$ and $\ell_{\max} = 1$. These values also show that the charge-flow contribution has an incomplete but non-negligible contribution to the isotropic polarizability. As mentioned above, the charge-

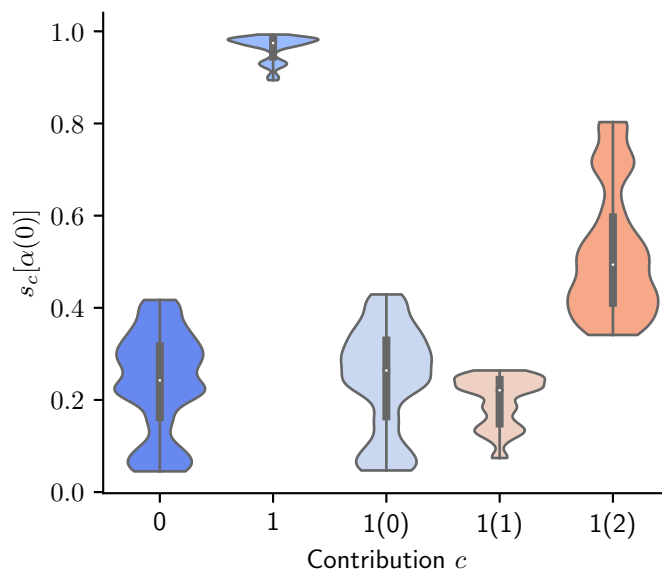


FIG. 2. Violin plots of the distribution of the isotropic descriptor for the static polarizability, $s_c[\alpha(0)]$, for all TS42 molecules, grouped by contribution c , as documented in Table II.

flow contribution reported here is typically smaller than in some previous works.^{41,42,53} This difference arises from the distinct definitions of charge flow and the AIM schemes applied in prior studies, as detailed in Section II.

The average $s_1[\alpha(0)]$ value (0.964) approaches 1.0, indicating that the molecular dipole polarizability can be accurately predicted by considering both atomic fluctuating charges and dipoles. Such results are in accordance with previous research^{71,72}. The charge-dipole contribution, $s_{1(1)}[\alpha(0)]$, is generally limited, yielding an average value of 0.197, while the dipole-only contribution has the main contribution with an average value of 0.520. Violin plots of $s_c[\alpha(\omega)]$ for other frequencies can be found in Figure S1.

Figure 3 further explores the dependence of $s_{1(0)}[\alpha(\omega)]$, $s_{1(1)}[\alpha(\omega)]$, and $s_{1(2)}[\alpha(\omega)]$ on the imaginary frequency. We observe a slight increase in the contribution of charge-flow with increasing $|\omega|$, except for the highest frequency. Interestingly, a similar trend can be identified in the dipole-only contribution, where the increase is more pronounced than in the charge-flow case. Considering that the sum of charge-flow, dipole-only, and charge-dipole contributions nearly equals unity, the charge-dipole contribution, $s_{1(1)}[\alpha(\omega)]$, decreases with increasing $|\omega|$ as depicted in Figure 3, attaining a negative average value when $|\omega| \geq 2.308$. As $|\omega|$ increases, the difference between charge-flow and dipole-only contributions

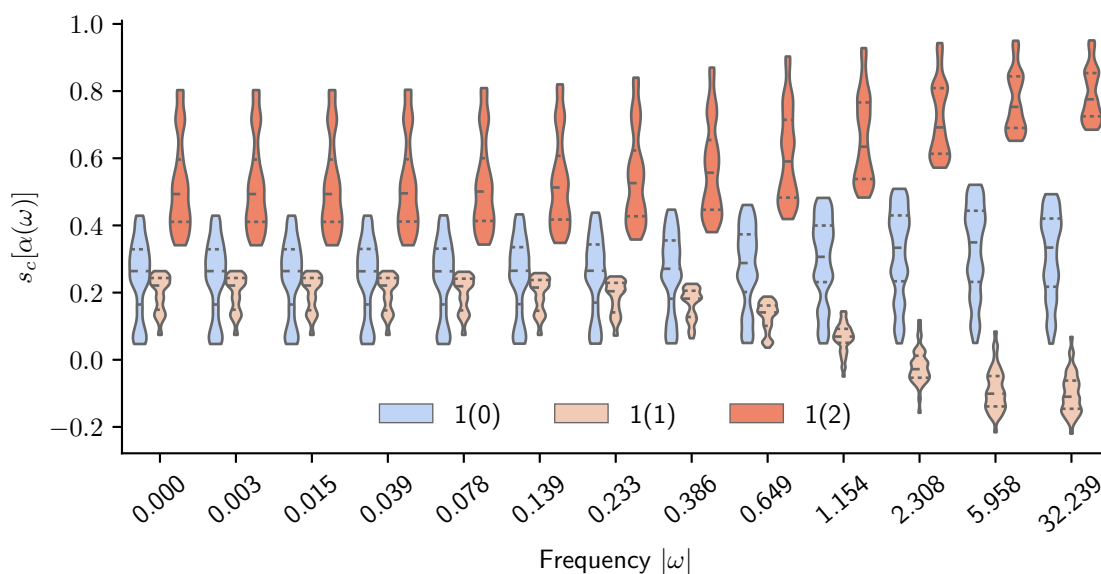


FIG. 3. The dependence on the frequency of the isotropic descriptor for the polarizability, $s_c[\alpha(\omega)]$, for the charge-flow [$c = 1(0)$] charge-dipole [$c = 1(1)$] and dipole-only [$c = 1(2)$], contributions.

also increases, causing the contribution of charge-flow to fall below that of dipole-only in high-frequency cases for all molecules when $|\omega| \geq 1.154$. Overall, the frequency dependence is small and the role of charge-flow remains comparable over the entire range of tested frequencies.

Figure 4 presents scatter plots of $s_{1(0)}[\alpha(0)]$ and $s_{1(2)}[\alpha(0)]$ as a function of the number of non-hydrogen atoms. We note that the contribution of charge-flow increases with the number of non-hydrogen atoms, while that of dipole-only decreases. This trend also holds for nonzero frequencies, as shown in Figure S2. In the static case, the contribution of charge-flow overtakes that of dipole-only when the number of non-hydrogen atoms in the TS42 database exceeds 5. For small molecules, most notably HF, HCl, and HBr, the isotropic dipole-only descriptor, $s_{1(2)}[\alpha(0)]$, is close to 1, while other contributions remain negligible. This is likely due to the limited number of non-hydrogen atoms in these molecules, which restricts charge exchange between atoms. Molecules with longer chains (e.g., C_6H_{14} , C_7H_{16} , and C_8H_{18}) or π -conjugated systems (e.g., C_6H_6), have the largest charge-flow contributions. This can be traced back to the larger number of non-hydrogen atoms in these molecules and the delocalized bonds, which are known to be highly polarizable. These results confirm that charge-flow varies with molecular topology and chemical bonding, which is consistent with

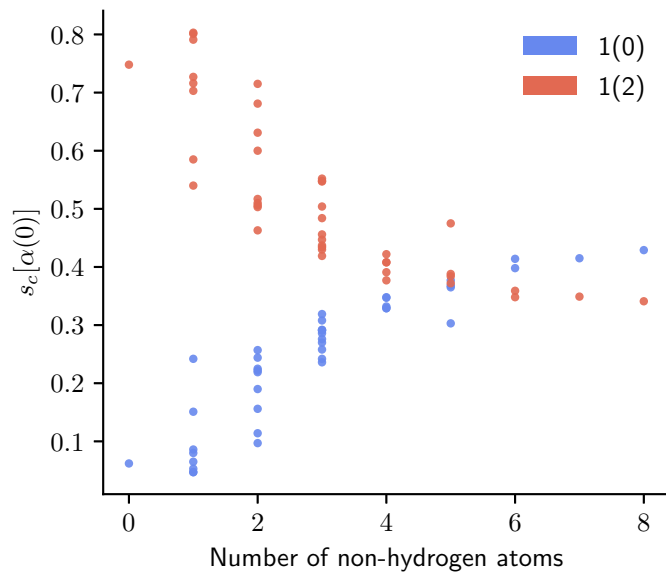


FIG. 4. The distributions of the isotropic descriptor for the static polarizability, $s_c[\alpha(0)]$, for the charge-flow [$c = 1(0)$] and dipole-only [$c = 1(2)$] contributions, grouped by the number of non-hydrogen atoms in the TS42 molecules.

the use of atom-condensed response kernels for the characterization of chemical bonding.⁴⁴

B. Anisotropy of dipole polarizability

Table IV details the $u_c^{\parallel}[\alpha(0)]$ values of (static) anisotropic polarizability. Tables S13-S24 show analogous results for other frequencies. Figure 5 depicts violin plots of the $u_c^{\parallel}[\alpha(0)]$ values for different contributions c . Similar violin plots of $u_c^{\parallel}[\alpha(\omega)]$ at higher frequencies can be found in Figure S3. In addition, the results of $\|\alpha_c(\omega)\|$ for all frequencies studied are presented in Tables S25-S37.

The average values of $u_0^{\parallel}[\alpha(0)]$ (0.032) and $u_{1(0)}^{\parallel}[\alpha(0)]$ (0.034) are close to the reference result $u_{\text{ref}}[\alpha(0)]$ (0.035). Both approaches to isolate the charge-flow contribution are again consistent. The reference is qualitatively reproduced by the charge-flow result, meaning that charge-flow contributions can explain most of the anisotropy of the static dipole polarizability. One average, the charge-dipole and dipole-dipole effects also contribute, but compensate each other to large extent.

The descriptor $u_c^{\parallel}[\alpha]$ is designed to have a meaningful sign that reveals whether contri-

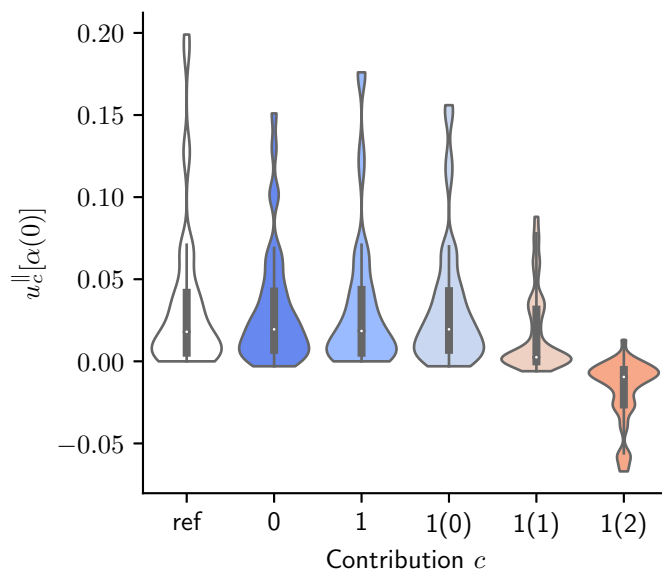


FIG. 5. Violin plots of anisotropic descriptor of the static dipole polarizability, $u_c^{\parallel}[\alpha(0)]$ for all molecules in TS42, grouped by contribution c , as documented in Table II.

bution c is pointing in the right direction. However, a good correspondence between $u_c^{\parallel}[\alpha]$ and $u_{\text{ref}}^{\parallel}[\alpha]$ is only a necessary condition for contribution c to fully explain the reference. Because this descriptor is defined through a scalar product, it is insensitive to contributions orthogonal to the reference. To further support our claim that the anisotropy is qualitatively reproduced by the charge-flow contribution, we verified that the following inequality holds for all molecules and all imaginary frequencies up to $0.386 \times i$:

$$\frac{\|\vec{\alpha}_{1(0)}(\omega) - \vec{\alpha}(\omega)\|^2}{\|\vec{\alpha}(\omega)\|^2 + (\alpha^{\text{iso}}(\omega))^2} \leq 0.02 \quad (26)$$

The term $(\alpha^{\text{iso}}(\omega))^2$ in the denominator is included to avoid (near) division by zero for molecules lacking anisotropy in the reference calculation. For imaginary frequencies with larger magnitude, the charge-flow and other contributions do not vanish as quickly, as mentioned in the previous paragraph, thereby making larger relative errors.

All $u_0^{\parallel}[\alpha(0)]$ and $u_{1(0)}^{\parallel}[\alpha(0)]$ values are positive, while all $u_{1(2)}^{\parallel}[\alpha(0)]$ values are negative, except for NH_3 and H_2S . Like other molecules with a single non-hydrogen atom, these two are only weakly anisotropic. Unlike other molecules, the charge-flow and charge-dipole contributions to the anisotropy have the wrong sign. These aberrations could be due to the presence of lone pairs, whose contribution is local within the non-hydrogen atom, such that

charge-flow models should not be expected to perform well for these specific cases.

Notably, the charge-flow contribution significantly influences the anisotropic polarizability of molecules with highly polarizable bonds, typically delocalized, double or tripple bonds For example, these are present in the molecules CS_2 , N_2 , COS , CO_2 , C_6H_6 , and C_2H_2 . For such molecules, $u_{1(2)}^{\parallel}[\alpha(0)]$ also contributes significantly, but with the opposite sign. The large contributions with opposite sign may pose challenges when parametrizing an approximate polarizable force field. Due to the cancellation of different effects, small absolute errors on individual contributions would be needed to obtain a small relative error on the combined result.

Figure 6 examines the dependence of $u_{1(0)}^{\parallel}[\alpha(\omega)]$ and $u_{\text{ref}}^{\parallel}[\alpha(\omega)]$ on the imaginary frequency ω . It can be observed that with increasing $|\omega|$, the anisotropy of the TD-DFT reference decreases and becomes very small at high frequencies ($|\omega| \geq 2.308$). Tables S25-S37 show in more detail how the anisotropy disappears at high frequency for individual molecules. This behavior is reproduced quantitatively by the ACKS2 ω model with $\ell_{\text{max}} = 1$. (See figure S3.) The charge-flow contribution follows this trend closely, but does not drop as sharply to zero at higher frequencies. In this regime, some molecules, e.g. C_2H_2 , C_6H_6 , and CO_2 , have relatively large contributions $c = "1(0)"$ and $c = "1(2)"$, adding up to a much smaller total anisotropy, as shown in Tables S22-S24. Also here, quantitative results rely on compensation effects between different terms, which may be challenging to reproduce with more approximate models.

C. C_6 coefficients

Figure 7(a) displays violin plots of the distribution of $s_c[C_6]$ over all molecular pairs, for each contribution c . In Figure 3, $s_0[\alpha(\omega)]$ shows a mild dependency on frequency. We can use this weak frequency dependency to approximate $s_0[C_6]$ in terms of $s_0[\alpha(\omega)]$ by rewriting Eq. (20) as:

$$s_0^{AB}[C_6] \approx \int_0^{\infty} s_0^A[\alpha(iv)]s_0^B[\alpha(iv)]dv, \quad (27)$$

where $s_0^{AB}[C_6]$ is the $s_0[C_6]$ value of molecular pair A and B, and $s_0^{A(B)}[\alpha(iv)]$ are the $s_0[\alpha(iv)]$ values for molecule A (B). Our results indicate that charge-flow contributions to C_6 are relatively small, with very similar trends observed for $c = 0$ and $c = 1(00)$. The small magnitude

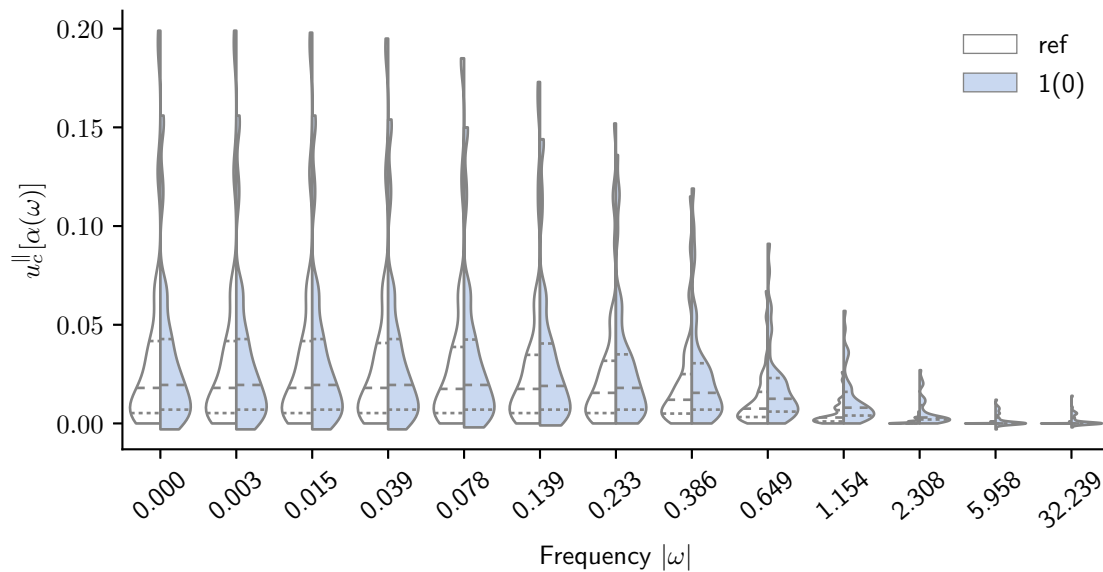


FIG. 6. The dependence on the frequency of the anisotropic descriptor for the polarizability, $u_c^{\parallel}[\alpha(\omega)]$, for the charge-flow contribution [$c = 1(0)$] and the reference [$c = \text{ref}$].

of charge-flow dispersion emerges from the underestimation of the isotropic dipole polarizability across all frequencies by the charge-flow contribution. This underestimation is amplified in the isotropic C_6 coefficient because it scales quadratically with the dipole polarizability. The dipole-only contribution, $c = 1(22)$, is in general the largest, but other contributions involving fluctuating charges and dipoles are also needed to obtain a quantitative reproduction of the reference result. These findings align with previous work.⁷²

Figure 8 illustrates the dependence of the largest $s_{1(00)}[C_6]$ values on the number of non-hydrogen atoms in the molecular dimer. The corresponding detailed data are shown in Table V. Charge-flow effects have an increasing contribution to the isotropic C_6 of larger molecular pairs, in line with our results for the isotropic polarizability.

Figure 7(b) presents violin plots of the distribution of $u_c^{\parallel}[C_6]$ values over all molecular pairs in TS42, for each contribution c . The charge-flow contribution to anisotropic dispersion is on average 0.066 for $u_0^{\parallel}[C_6]$ and 0.069 for $u_{1(00)}^{\parallel}[C_6]$. Again, both characterizations of charge-flow agree with each other. Whereas charge-flow could explain most of the anisotropy of the dipole polarizability, it cannot accomplish the same for dispersion. This can be understood by analyzing Eq. (19): some of the anisotropic dispersion coefficients depend on the isotropic frequency dependent polarizability of one of the two molecules. As discussed in Section IV A,

This is the author's peer reviewed, accepted manuscript. However, the online version of record will be different from this version once it has been copyedited and typeset.
PLEASE CITE THIS ARTICLE AS DOI: 10.1063/5.0163842

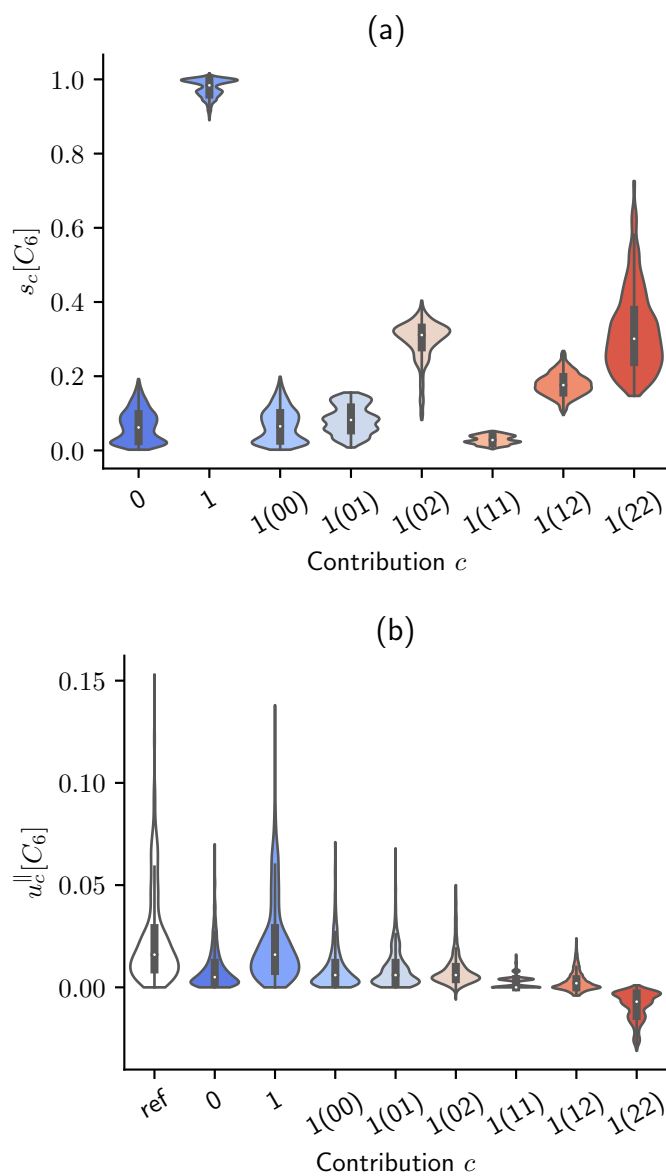


FIG. 7. Violin plots of the isotropic descriptor for dispersion coefficients, $s_c[C_6]$ (panel a), and the anisotropic descriptor, $u_c^{\parallel}[C_6]$ (panel b), for all molecular pairs from the TS42 database, for each category c , as documented in Table II.

this isotropic contribution is not reproduced qualitatively when only considering charge-flow. Nonetheless, $u_0^{\parallel}[C_6]$ remains significant for several molecular pairs, and we list the top 50 in Table VI. The minor discrepancy between the distribution of $u_{\text{ref}}^{\parallel}[C_6]$ and $u_1^{\parallel}[C_6]$ values suggests that anisotropic C_6 coefficients can be accurately represented by combining frequency-dependent fluctuating charges and dipoles.

This is the author's peer reviewed, accepted manuscript. However, the online version of record will be different from this version once it has been copyedited and typeset.

PLEASE CITE THIS ARTICLE AS DOI: 10.1063/5.0163842

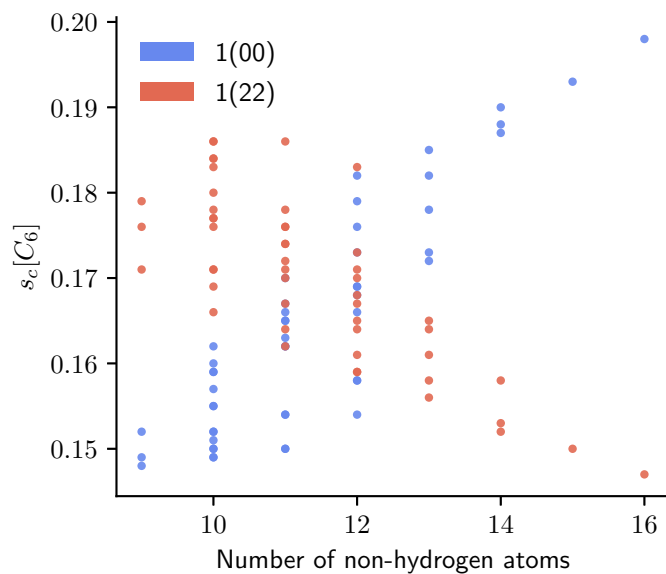


FIG. 8. The dependence on the number of non-hydrogen atoms of the 50 highest charge-flow isotropic descriptors for the C_6 dispersion coefficient, $s_{1(00)}[C_6]$. For the same molecular pairs, also the corresponding dipole-only descriptor [$c = 1(22)$] is included.

Finally, it is noteworthy that the dipole-only contribution to the anisotropy, $u_{1(22)}^{\parallel}[C_6]$, is negative in general. This suggests that fluctuating dipoles render the dispersion more isotropic, countering the anisotropy from all other contributions.

This is the author's peer reviewed, accepted manuscript. However, the online version of record will be different from this version once it has been copyedited and typeset.
PLEASE CITE THIS ARTICLE AS DOI: 10.1063/5.0163842

TABLE IV. Anisotropic descriptors $u_c^{\parallel}[\alpha(0)]$ for all molecules in the TS42 database, for each contribution c , as documented in Table II.

Molecule	$u_{\text{ref}}^{\parallel}[\alpha(0)]$	$u_0^{\parallel}[\alpha(0)]$	$u_1^{\parallel}[\alpha(0)]$	$u_{1(0)}^{\parallel}[\alpha(0)]$	$u_{1(1)}^{\parallel}[\alpha(0)]$	$u_{1(2)}^{\parallel}[\alpha(0)]$
CS ₂	0.199	0.151	0.176	0.156	0.078	-0.058
N ₂ O	0.187	0.130	0.173	0.149	0.088	-0.064
CO ₂	0.132	0.102	0.128	0.123	0.072	-0.067
COS	0.123	0.101	0.116	0.112	0.060	-0.056
C ₆ H ₆	0.061	0.069	0.064	0.070	0.034	-0.041
C ₂ H ₂	0.067	0.065	0.071	0.067	0.062	-0.058
SO ₂	0.070	0.060	0.066	0.066	0.028	-0.028
Cl ₂	0.071	0.057	0.059	0.057	0.038	-0.037
C ₈ H ₁₈	0.034	0.051	0.034	0.051	-0.002	-0.015
C ₃ H ₆	0.041	0.045	0.042	0.047	0.018	-0.023
C ₇ H ₁₆	0.029	0.043	0.029	0.043	-0.000	-0.013
C ₂ H ₄	0.042	0.041	0.044	0.042	0.030	-0.028
H ₂ CO	0.052	0.036	0.052	0.039	0.038	-0.024
C ₆ H ₁₄	0.024	0.036	0.024	0.037	-0.000	-0.012
CH ₃ CHO	0.033	0.028	0.032	0.031	0.014	-0.014
N ₂	0.036	0.027	0.039	0.030	0.038	-0.030
CH ₃ CH ₂ OCH ₂ CH ₃	0.019	0.028	0.019	0.028	0.000	-0.009
C ₅ H ₁₂	0.018	0.027	0.018	0.027	0.000	-0.010
C ₄ H ₁₀ O	0.018	0.027	0.018	0.027	0.002	-0.011
CH ₃ COCH ₃	0.022	0.021	0.022	0.022	0.008	-0.009
C ₄ H ₁₀	0.013	0.020	0.013	0.020	0.001	-0.008
CH ₃ CH ₃ CH ₃ N	0.014	0.019	0.014	0.019	0.002	-0.007
C ₃ H ₇ OH	0.012	0.018	0.012	0.018	0.002	-0.009
H ₂	0.043	0.018	0.044	0.018	0.052	-0.027
CO	0.016	0.016	0.019	0.017	0.022	-0.020
CH ₃ OCH ₃	0.010	0.016	0.011	0.016	0.002	-0.008
HF	0.031	0.011	0.027	0.012	0.032	-0.017
CH ₃ NHCH ₃	0.008	0.011	0.008	0.011	0.002	-0.005
C ₂ H ₅ OH	0.007	0.010	0.007	0.010	0.002	-0.006
C ₃ H ₈	0.006	0.009	0.006	0.009	0.002	-0.004
CH ₃ OH	0.005	0.007	0.005	0.007	0.003	-0.005
CH ₃ NH ₂	0.006	0.007	0.006	0.007	0.002	-0.004
C ₂ H ₆	0.005	0.007	0.005	0.007	0.000	-0.003
C ₄ H ₈	0.004	0.006	0.004	0.006	0.000	-0.001
HCl	0.005	0.004	0.005	0.005	0.008	-0.007
HBr	0.003	0.004	0.003	0.004	0.006	-0.007
H ₂ O	0.002	0.002	0.002	0.002	0.006	-0.006
CH ₄	0.000	-0.000	0.000	0.000	0.000	-0.000
CCl ₄	0.000	0.000	0.000	-0.000	0.000	0.000
SiH ₄	0.000	0.000	-0.000	0.000	0.000	-0.000
H ₂ S	0.000	-0.001	-0.000	-0.001	-0.000	0.001
NH ₃	0.005	-0.003	0.004	-0.003	-0.006	0.013
Min.	0.000	-0.003	-0.000	-0.003	-0.006	-0.067
Max.	0.199	0.151	0.176	0.156	0.088	0.013
Mean	0.035	0.032	0.034	0.034	0.018	-0.018

This is the author's peer reviewed, accepted manuscript. However, the online version of record will be different from this version once it has been copyedited and typeset.
 PLEASE CITE THIS ARTICLE AS DOI: 10.1063/5.0163842

TABLE V. Isotropic descriptors $s_c[C_6]$ for the 50 molecular pairs from TS42 with the highest $s_{1(00)}[C_6]$ value.

Molecule	$s_0[C_6]$	$s_1[C_6]$	$s_{1(00)}[C_6]$	$s_{1(01)}[C_6]$	$s_{1(02)}[C_6]$	$s_{1(11)}[C_6]$	$s_{1(12)}[C_6]$	$s_{1(22)}[C_6]$
C ₈ H ₁₈ ...C ₈ H ₁₈	0.192	1.002	0.198	0.156	0.340	0.036	0.128	0.147
C ₈ H ₁₈ ...C ₇ H ₁₆	0.187	1.002	0.193	0.154	0.339	0.036	0.132	0.150
C ₈ H ₁₈ ...C ₆ H ₆	0.186	0.995	0.190	0.144	0.346	0.032	0.126	0.158
C ₇ H ₁₆ ...C ₇ H ₁₆	0.182	1.001	0.188	0.152	0.338	0.036	0.132	0.152
C ₈ H ₁₈ ...C ₆ H ₁₄	0.181	1.001	0.187	0.154	0.337	0.036	0.134	0.153
C ₆ H ₆ ...C ₇ H ₁₆	0.182	0.995	0.185	0.144	0.344	0.032	0.128	0.161
C ₇ H ₁₆ ...C ₆ H ₁₄	0.176	1.001	0.182	0.154	0.336	0.036	0.136	0.156
C ₆ H ₆ ...C ₆ H ₆	0.181	0.988	0.182	0.136	0.350	0.028	0.124	0.170
C ₆ H ₁₄ ...C ₆ H ₆	0.175	0.995	0.179	0.142	0.342	0.032	0.134	0.165
C ₅ H ₁₂ ...C ₈ H ₁₈	0.172	1.001	0.178	0.152	0.336	0.036	0.138	0.158
C ₆ H ₁₄ ...C ₆ H ₁₄	0.170	1.001	0.176	0.152	0.334	0.040	0.140	0.159
C ₇ H ₁₆ ...C ₅ H ₁₂	0.168	1.001	0.173	0.152	0.334	0.040	0.142	0.161
C ₈ H ₁₈ ...CH ₃ CH ₂ OCH ₂ CH ₃	0.169	1.001	0.173	0.148	0.340	0.036	0.140	0.165
C ₈ H ₁₈ ...C ₄ H ₁₀ O	0.167	1.001	0.172	0.150	0.337	0.036	0.140	0.164
C ₆ H ₆ ...C ₅ H ₁₂	0.167	0.995	0.170	0.144	0.340	0.036	0.138	0.170
CH ₃ CH ₂ OCH ₂ CH ₃ ...C ₇ H ₁₆	0.164	1.001	0.169	0.146	0.337	0.036	0.142	0.168
C ₄ H ₈ ...C ₈ H ₁₈	0.165	0.999	0.169	0.156	0.330	0.040	0.146	0.159
C ₄ H ₁₀ O...C ₇ H ₁₆	0.163	1.001	0.168	0.150	0.336	0.036	0.142	0.167
C ₆ H ₁₄ ...C ₅ H ₁₂	0.162	1.001	0.167	0.152	0.331	0.040	0.146	0.164
C ₈ H ₁₈ ...C ₄ H ₁₀	0.161	1.001	0.166	0.152	0.333	0.040	0.146	0.164
CH ₃ CH ₂ OCH ₂ CH ₃ ...C ₆ H ₆	0.163	0.994	0.166	0.138	0.343	0.032	0.136	0.178
C ₆ H ₆ ...C ₄ H ₁₀ O	0.162	0.995	0.165	0.140	0.341	0.032	0.140	0.176
C ₄ H ₈ ...C ₇ H ₁₆	0.160	0.999	0.165	0.154	0.328	0.040	0.148	0.162
C ₆ H ₁₄ ...CH ₃ CH ₂ OCH ₂ CH ₃	0.159	1.001	0.163	0.146	0.335	0.036	0.146	0.172
C ₄ H ₈ ...C ₆ H ₆	0.159	0.993	0.162	0.146	0.333	0.036	0.144	0.171
C ₇ H ₁₆ ...C ₄ H ₁₀	0.157	1.001	0.162	0.152	0.332	0.040	0.148	0.167
C ₄ H ₁₀ O...C ₆ H ₁₄	0.157	1.001	0.162	0.148	0.332	0.040	0.146	0.171
C ₅ H ₁₂ ...C ₅ H ₁₂	0.155	1.001	0.160	0.152	0.328	0.040	0.152	0.169
C ₄ H ₈ ...C ₆ H ₁₄	0.155	0.999	0.159	0.154	0.326	0.044	0.152	0.166
C ₄ H ₁₀ ...C ₆ H ₆	0.156	0.994	0.159	0.144	0.336	0.036	0.144	0.177
C ₈ H ₁₈ ...CH ₃ CH ₃ CH ₃ N	0.153	1.002	0.158	0.150	0.335	0.040	0.150	0.171
C ₃ H ₇ OH...C ₈ H ₁₈	0.154	1.001	0.158	0.148	0.336	0.040	0.146	0.173
C ₆ H ₁₄ ...C ₄ H ₁₀	0.152	1.001	0.157	0.150	0.328	0.040	0.152	0.171
C ₅ H ₁₂ ...C ₄ H ₁₀ O	0.150	1.001	0.155	0.146	0.329	0.040	0.154	0.176
C ₅ H ₁₂ ...CH ₃ CH ₂ OCH ₂ CH ₃	0.151	1.000	0.155	0.146	0.332	0.040	0.150	0.177
CH ₃ COCH ₃ ...C ₈ H ₁₈	0.148	0.997	0.154	0.138	0.345	0.036	0.144	0.183
CH ₃ CH ₃ CH ₃ N...C ₇ H ₁₆	0.149	1.002	0.154	0.148	0.332	0.040	0.154	0.174
C ₇ H ₁₆ ...C ₃ H ₇ OH	0.150	1.001	0.154	0.146	0.334	0.040	0.150	0.176
C ₃ H ₇ OH...C ₆ H ₆	0.149	0.994	0.152	0.138	0.338	0.036	0.144	0.186
CH ₃ CH ₃ CH ₃ N...C ₆ H ₆	0.149	0.995	0.152	0.140	0.337	0.036	0.148	0.184
C ₅ H ₁₂ ...C ₄ H ₈	0.148	0.999	0.152	0.152	0.322	0.044	0.158	0.171
CH ₃ CH ₂ OCH ₂ CH ₃ ...CH ₃ CH ₂ OCH ₂ CH ₃	0.148	1.000	0.151	0.140	0.334	0.036	0.152	0.186
C ₄ H ₁₀ O...CH ₃ CH ₂ OCH ₂ CH ₃	0.147	1.000	0.150	0.142	0.333	0.040	0.152	0.184
C ₄ H ₁₀ O...C ₄ H ₁₀ O	0.145	1.000	0.150	0.144	0.330	0.040	0.156	0.183
C ₇ H ₁₆ ...CH ₃ COCH ₃	0.144	0.997	0.150	0.136	0.341	0.036	0.148	0.186
C ₃ H ₈ ...C ₈ H ₁₈	0.145	1.000	0.150	0.150	0.331	0.040	0.154	0.174
C ₆ H ₁₄ ...CH ₃ CH ₃ CH ₃ N	0.144	1.002	0.149	0.148	0.329	0.040	0.158	0.178
C ₆ H ₁₄ ...C ₃ H ₇ OH	0.145	1.000	0.149	0.146	0.330	0.040	0.156	0.180
C ₄ H ₁₀ ...C ₅ H ₁₂	0.145	1.000	0.149	0.148	0.325	0.044	0.160	0.176
CH ₃ CH ₂ OCH ₂ CH ₃ ...C ₄ H ₈	0.145	0.999	0.148	0.146	0.325	0.044	0.158	0.179
...
Min.	0.002	0.890	0.002	0.008	0.082	0.004	0.096	0.147
Max.	0.192	1.016	0.198	0.156	0.403	0.052	0.268	0.726
Mean	0.066	0.977	0.069	0.083	0.297	0.028	0.178	0.322

This is the author's peer reviewed, accepted manuscript. However, the online version of record will be different from this version once it has been copyedited and typeset. PLEASE CITE THIS ARTICLE AS DOI: 10.1063/5.0163842

TABLE VI. Anisotropic descriptors $u_c^{\parallel}[C_6]$ for the 50 molecular pairs from TS42 with the highest $u_{1(00)}^{\parallel}[C_6]$ value.

Molecule	$u_{ref}^{\parallel}[C_6]$	$u_0^{\parallel}[C_6]$	$u_1^{\parallel}[C_6]$	$u_{1(00)}^{\parallel}[C_6]$	$u_{1(01)}^{\parallel}[C_6]$	$u_{1(02)}^{\parallel}[C_6]$	$u_{1(11)}^{\parallel}[C_6]$	$u_{1(12)}^{\parallel}[C_6]$	$u_{1(22)}^{\parallel}[C_6]$
CS ₂ ...CS ₂	0.153	0.070	0.131	0.071	0.056	0.010	0.012	0.004	-0.023
N ₂ O...CS ₂	0.151	0.065	0.134	0.070	0.060	0.009	0.016	0.004	-0.024
N ₂ O...N ₂ O	0.151	0.061	0.138	0.070	0.068	0.006	0.016	0.004	-0.024
CO ₂ ...CS ₂	0.121	0.052	0.110	0.059	0.050	0.010	0.012	0.004	-0.025
CO ₂ ...N ₂ O	0.124	0.050	0.115	0.059	0.056	0.008	0.016	0.004	-0.026
COS...CS ₂	0.119	0.052	0.105	0.056	0.042	0.015	0.008	0.006	-0.024
N ₂ O...COS	0.122	0.050	0.111	0.056	0.048	0.014	0.012	0.006	-0.025
N ₂ O...C ₆ H ₆	0.095	0.050	0.091	0.054	0.046	-0.002	0.012	0.000	-0.018
CS ₂ ...C ₆ H ₆	0.090	0.052	0.083	0.052	0.038	0.001	0.008	0.000	-0.017
CO ₂ ...CO ₂	0.100	0.040	0.094	0.049	0.048	0.010	0.012	0.004	-0.027
CO ₂ ...COS	0.097	0.040	0.089	0.047	0.040	0.014	0.008	0.006	-0.026
N ₂ O...C ₈ H ₁₈	0.080	0.042	0.077	0.045	0.032	0.007	0.004	0.002	-0.014
C ₆ H ₆ ...CO ₂	0.073	0.040	0.071	0.045	0.038	-0.002	0.008	0.000	-0.018
CS ₂ ...C ₈ H ₁₈	0.074	0.043	0.068	0.044	0.026	0.008	0.004	0.000	-0.013
COS...COS	0.093	0.039	0.084	0.044	0.032	0.016	0.008	0.008	-0.025
N ₂ O...C ₇ H ₁₆	0.078	0.039	0.074	0.042	0.030	0.008	0.004	0.004	-0.015
COS...C ₆ H ₆	0.068	0.039	0.064	0.041	0.032	0.002	0.008	0.002	-0.018
CS ₂ ...C ₇ H ₁₆	0.071	0.040	0.066	0.041	0.024	0.009	0.004	0.000	-0.013
N ₂ O...C ₂ H ₂	0.100	0.038	0.095	0.040	0.048	0.012	0.016	0.006	-0.027
C ₂ H ₂ ...CS ₂	0.094	0.039	0.087	0.039	0.044	0.013	0.012	0.006	-0.026
N ₂ O...C ₆ H ₁₄	0.076	0.036	0.072	0.039	0.030	0.009	0.004	0.004	-0.015
CS ₂ ...SO ₂	0.089	0.035	0.079	0.038	0.028	0.022	0.008	0.006	-0.021
N ₂ O...SO ₂	0.094	0.034	0.087	0.038	0.032	0.023	0.008	0.010	-0.023
C ₈ H ₁₈ ...CO ₂	0.060	0.033	0.058	0.037	0.026	0.005	0.004	0.000	-0.014
CS ₂ ...C ₆ H ₁₄	0.069	0.037	0.064	0.037	0.024	0.010	0.004	0.000	-0.013
C ₃ H ₆ ...N ₂ O	0.081	0.033	0.077	0.036	0.034	0.013	0.008	0.004	-0.019
CH ₃ CH ₂ OCH ₂ CH ₃ ...N ₂ O	0.073	0.032	0.070	0.035	0.026	0.012	0.004	0.006	-0.016
CS ₂ ...C ₃ H ₆	0.075	0.034	0.069	0.035	0.028	0.014	0.008	0.002	-0.017
C ₅ H ₁₂ ...N ₂ O	0.073	0.032	0.069	0.035	0.028	0.011	0.008	0.004	-0.015
C ₆ H ₆ ...C ₆ H ₆	0.045	0.035	0.046	0.035	0.024	-0.006	0.004	-0.004	-0.012
C ₈ H ₁₈ ...COS	0.054	0.032	0.051	0.034	0.020	0.007	0.004	-0.002	-0.012
CO ₂ ...C ₂ H ₂	0.077	0.030	0.075	0.034	0.040	0.011	0.012	0.006	-0.028
N ₂ O...C ₄ H ₁₀ O	0.073	0.032	0.069	0.034	0.028	0.011	0.008	0.004	-0.016
CO ₂ ...C ₇ H ₁₆	0.058	0.031	0.056	0.034	0.024	0.005	0.004	0.002	-0.014
CS ₂ ...C ₄ H ₁₀ O	0.065	0.032	0.060	0.033	0.024	0.012	0.004	0.000	-0.014
CS ₂ ...C ₅ H ₁₂	0.065	0.033	0.060	0.033	0.024	0.012	0.004	0.002	-0.013
CH ₃ CH ₂ OCH ₂ CH ₃ ...CS ₂	0.066	0.033	0.061	0.033	0.022	0.013	0.004	0.002	-0.014
C ₇ H ₁₆ ...COS	0.052	0.030	0.049	0.032	0.020	0.008	0.004	-0.002	-0.012
C ₆ H ₁₄ ...CO ₂	0.056	0.028	0.054	0.032	0.024	0.006	0.004	0.002	-0.014
CO ₂ ...SO ₂	0.072	0.027	0.068	0.032	0.026	0.019	0.004	0.008	-0.023
COS...C ₂ H ₂	0.072	0.030	0.068	0.031	0.034	0.013	0.008	0.008	-0.026
C ₄ H ₁₀ ...N ₂ O	0.070	0.029	0.067	0.031	0.026	0.013	0.008	0.006	-0.016
N ₂ O...C ₂ H ₄	0.083	0.029	0.079	0.031	0.036	0.017	0.012	0.008	-0.022
CH ₃ COCH ₃ ...N ₂ O	0.072	0.027	0.069	0.030	0.026	0.016	0.008	0.006	-0.017
Cl ₂ ...N ₂ O	0.093	0.028	0.081	0.030	0.028	0.028	0.008	0.014	-0.027
N ₂ O...C ₃ H ₇ OH	0.070	0.027	0.067	0.030	0.026	0.014	0.008	0.006	-0.016
CH ₃ CHO...N ₂ O	0.077	0.027	0.073	0.030	0.028	0.018	0.008	0.008	-0.019
CS ₂ ...C ₂ H ₄	0.077	0.030	0.071	0.030	0.030	0.017	0.008	0.004	-0.020
COS...SO ₂	0.067	0.027	0.062	0.030	0.020	0.020	0.004	0.006	-0.020
CS ₂ ...C ₄ H ₁₀	0.063	0.029	0.058	0.029	0.022	0.013	0.004	0.002	-0.014
...
Min.	0.000	0.000	0.000	0.000	0.000	-0.006	0.000	-0.004	-0.031
Max.	0.153	0.070	0.138	0.071	0.068	0.050	0.016	0.024	0.001
Mean	0.024	0.009	0.023	0.009	0.009	0.008	0.002	0.003	-0.009

V. DISCUSSION

While our findings demonstrate the relative importance of fluctuating charges in molecular polarizability and dispersion interactions, we acknowledge that there are alternative methods to accurately describe these phenomena without explicitly relying on charge-flow.⁸⁸ For example, many interaction models, such as polarizable force fields^{38,58,89–91} and dispersion corrections for DFT calculations,^{2,7,8,13,14,19,22,24,25,33,35,36} are motivated from a picture of dipole-polarizable atoms without charge-flow. Quantitative predictions made by such models imply that effects attributed to charge-flow in this work can also be reproduced with a different dipole-only model. This can be understood as follows. The distributed multipole analysis used here is only one way to decompose the molecular response kernel into separate contributions, and different atom-in-molecule partitioning schemes can be employed within this framework.^{69,74} Furthermore, response localization schemes can translate charge-flow effects into a dipole-only picture, explaining how dipole-only models can make quantitative predictions.⁶⁸ In addition, other approaches exist that can result in a quantitative dipole-only response model, e.g. by constructing complete response basis sets without monopolar terms⁹² or by transforming response functions to polarization densities.⁹³

One could even go a step further and consider decomposing the molecular electron density into different units than atoms in molecules. While it is uncommon to partition the density in contributions attributed to bonds, one can anticipate the result of such a hypothetical bond partitioning by treating a diatomic molecule as a single bond unit instead of partitioning it into two atoms. The results in Figure 1 illustrate this for carbon monoxide. When using atomic partitions, there is a significant charge-flow contribution to the polarizability. When treating this molecule as a single unit, there is no charge transfer to be observed and the response properties are all be attributed to the polarization of $\text{C}\equiv\text{O}$ bond unit.

All the ambiguities and choices discussed above will lead to a different perspective of what constitutes charge-flow, if any. In the literature, the importance of charge-flow is well established for long-range polarization in near-metallic extended systems.^{7,39–43,45–48} In addition, our numerical assessment confirms that the charge-flow contribution, as defined in this work, is related to non-local features, such as molecular geometry and chemical bonding, also in smaller molecules, such as those in the TS42 set.⁴⁴ Polarizable force fields and dispersion models may build on these relationships to parametrize charge-flow explicitly,

thereby improving their description of anisotropic response properties. In other words, we show that the charge flow is not only useful for modeling non-standard power laws in Type-C dispersion,¹⁵ but that it is also helpful for understanding anisotropic dispersion of isolated molecules.

VI. CONCLUSIONS

The impact of fluctuating charges on dynamic linear-response properties is investigated and numerically assessed with the TS42 dataset, comprising both organic and inorganic molecules. The dipole polarizability tensor is recoupled to easily separate isotropic and anisotropic components, which also allows for the definition of anisotropic C_6 dispersion coefficients. The recoupled properties are then used to define two descriptors (isotropic and anisotropic) for the charge-flow contribution to polarizability and dispersion. The molecular frequency-dependent polarizabilities are computed with the ACKS2 ω model, either with fluctuating charges only ($\ell_{\max} = 0$) or fluctuating charges and dipoles ($\ell_{\max} = 1$). In the latter case, charge-flow, charge-dipole, and dipole-only effects are easily separated. All ACKS2 ω parameters are derived from LDA/Aug-cc-pVDZ wavefunctions, and the response properties at this level of theory are used as a reference. Our tests reveal that the two ways to define the charge-flow contribution ($\ell_{\max} = 0$ or the charge-flow part of $\ell_{\max} = 1$) yield very similar results. In general, the $\ell_{\max} = 1$ model quantitatively reproduces all tested quantities: both isotropic and anisotropic polarizability and dispersion.

The results for the TS42 set show that charge-flow contributions alone significantly underestimate the molecular isotropic dipole polarizability, and that the dipole-only contribution is larger. Nevertheless, the charge-flow contribution is in general not negligible and its significance depends strongly on molecular geometry, the presence of polarizable bonds, and the number of non-hydrogen atoms. In long-chain or π -conjugated molecules, the charge-flow contribution can even exceed the dipole-only counterpart. Our results also reveal a weak dependence of the charge-flow contribution on frequency, whereas charge-dipole and dipole-only contributions respectively decrease and increase slightly with increasing magnitude of the imaginary frequency.

We also investigate the static anisotropic polarizability and its contributions across different frequencies. The results demonstrate that the charge-flow contribution alone reasonably

predicts the anisotropy of the polarizability. The overall anisotropy decreases with increasing magnitude of the imaginary frequency, and becomes negligible at the highest frequencies ($|\omega| \geq 2.308$). In this limit, polarizability becomes almost perfectly isotropic. Charge-flow and other contributions to the anisotropic polarizability follow the same decreasing trend in magnitude, except that they do not approach zero as closely at higher frequencies. In this limit, their residual contributions cancel each other out.

The analysis also reveals that the isotropic C_6 coefficients are considerably underestimated by charge-flow contributions alone. This discrepancy is the logical consequence of the noticeable underestimation of the isotropic dipole polarizability by charge-flow at all the frequencies employed in the C_6 computations. Charge-flow and charge-dipole effects still contribute significantly, but the dipole-only effect is larger.

Unlike the anisotropic polarizability, anisotropic dispersion is not fully reproduced by charge-flow contributions alone. The impact of charge-flow is not negligible, but other charge-dipole terms are also important. Remarkably, the dipole-only contribution generally reduces the dispersion anisotropy.

In conclusion, this research offers valuable insights into the leading contributors to molecular polarizability and C_6 coefficients, highlighting the significance of fluctuating charges in determining the dynamic linear-response properties of finite systems. Nevertheless, we acknowledge, existing interaction models without charge-flow, i.e. which rely exclusively atomic dipoles, have proven their effectiveness. This contrast remains fascinating as charge-flow contributions correlate with non-local features at a higher length scale than that of local atomic polarizabilities. Future (frequency-dependent) polarizable force fields could improve by including charge-flow effects and this work shows in which cases such improvements should be expected to be beneficial.

ACKNOWLEDGEMENTS

Y.C. and T.V. acknowledge the Foundation of Scientific Research - Flanders (FWO, file number G0A9717N) and the Research Board of Ghent University (BOF) for their financial support. The resources and services used in this work were provided by the VSC (Flemish Supercomputer Center), funded by the Research Foundation - Flanders (FWO) and the Flemish Government. We thank Dr. Jelle Vekeman for helpful comments on the manuscript.

DATASET AVAILABILITY STATEMENT

The data that support the findings of this study are openly available in “TS42 TD-DFT Dipole Polarizabilities as a function of imaginary frequency”, at <https://doi.org/10.5281/zenodo.8047106>, reference number 8047106.

SUPPLEMENTARY MATERIAL

The Supplementary Material is a PDF document containing:

- Violin plots of the distribution of $s_c[\alpha(\omega)]$ over the TS42 dataset, for all relevant contributions c , and for all imaginary frequencies used in this work.
- Scatter plots showing the dependence of the descriptors $s_{1(0)}[\alpha(\omega)]$ and $s_{1(2)}[\alpha(\omega)]$ on the number of non-hydrogen atoms in molecules, for all imaginary frequencies considered in this work.
- Violin plots of the distribution of the descriptor $u_c^{\parallel}[\alpha(\omega)]$ over the TS42 database, for all relevant contributions c and all imaginary frequencies considered in this work.
- Tables with numerical values of $s_c[\alpha(\omega)]$, $\|\vec{\alpha}_c\|$, $u_c^{\parallel}[\alpha(\omega)]$, for all molecules in TS42, for all relevant contributions c , and for all imaginary frequencies used in this work.

REFERENCES

- ¹Martin Stöhr, Troy Van Voorhis, and Alexandre Tkatchenko. Theory and practice of modeling van der Waals interactions in electronic-structure calculations. *Chem. Soc. Rev.*, 48(15):4118–4154, 2019.
- ²Stefan Grimme, Andreas Hansen, Jan Gerit Brandenburg, and Christoph Bannwarth. Dispersion-Corrected Mean-Field Electronic Structure Methods. *Chem. Rev.*, 116(9):5105–5154, 2016.
- ³Stefan Grimme and Christoph Bannwarth. Ultra-fast computation of electronic spectra for large systems by tight-binding based simplified Tamm-Dancoff approximation (sTDA-xTB). *J. Chem. Phys.*, 145(5):054103, 2016.

- ⁴János G. Ángyán, Iann C. Gerber, Andreas Savin, and Julien Toulouse. Van der Waals forces in density functional theory: Perturbational long-range electron-interaction corrections. *Phys. Rev. A*, 72(1):012510, 2005.
- ⁵Kristian Berland, Valentino R. Cooper, Kyuho Lee, Elsebeth Schröder, T. Thonhauser, Per Hyldgaard, and Bengt I. Lundqvist. Van der Waals forces in density functional theory: A review of the vdW-DF method. *Rep. Prog. Phys.*, 78(6):066501, 2015.
- ⁶A. D. Buckingham, P. W. Fowler, and Jeremy M. Hutson. Theoretical studies of van der Waals molecules and intermolecular forces. *Chem. Rev.*, 88(6):963–988, 1988.
- ⁷Jan Hermann, Robert A. Jr. DiStasio, and Alexandre Tkatchenko. First-Principles Models for van der Waals Interactions in Molecules and Materials: Concepts, Theory, and Applications. *Chem. Rev.*, 117(6):4714–4758, 2017.
- ⁸L. M. Woods, D. A. R. Dalvit, A. Tkatchenko, P. Rodriguez-Lopez, A. W. Rodriguez, and R. Podgornik. Materials perspective on Casimir and van der Waals interactions. *Rev. Mod. Phys.*, 88(4):045003, 2016.
- ⁹Peng Xu, Melisa Alkan, and Mark S. Gordon. Many-Body Dispersion. *Chem. Rev.*, 120(22):12343–12356, 2020.
- ¹⁰F. London. Zur Theorie und Systematik der Molekularkräfte. *Z. Physik*, 63(3):245–279, 1930.
- ¹¹E. Zaremba and W. Kohn. Van der Waals interaction between an atom and a solid surface. *Phys. Rev. B*, 13(6):2270–2285, 1976.
- ¹²Axel D. Becke and Erin R. Johnson. Exchange-hole dipole moment and the dispersion interaction revisited. *J. Chem. Phys.*, 127(15):154108, 2007.
- ¹³Alexandre Tkatchenko and Matthias Scheffler. Accurate Molecular Van Der Waals Interactions from Ground-State Electron Density and Free-Atom Reference Data. *Phys. Rev. Lett.*, 102(7):073005, 2009.
- ¹⁴Stefan Grimme, Stephan Ehrlich, and Lars Goerigk. Effect of the damping function in dispersion corrected density functional theory. *J. Comput. Chem.*, 32(7):1456–1465, 2011.
- ¹⁵John F. Dobson. Beyond pairwise additivity in London dispersion interactions. *Int. J. Quantum Chem.*, 114(18):1157–1161, 2014.
- ¹⁶Tim Gould, Sébastien Lebègue, János G. Ángyán, and Tomáš Bučko. A fractionally ionic approach to polarizability and van der waals many-body dispersion calculations. *J. Chem.*

Theory Comput., 12(12):5920–5930, 2016.

- ¹⁷A. Otero-de-la-Roza, Luc M. LeBlanc, and Erin R. Johnson. What is “many-body” dispersion and should I worry about it? *Phys. Chem. Chem. Phys.*, 22(16):8266–8276, 2020.
- ¹⁸John F. Dobson, Andreas Savin, János G. Ángyán, and Ru-Fen Liu. Spooky correlations and unusual van der waals forces between gapless and near-gapless molecules. *J. Chem. Phys.*, 145(20):204107, 2016.
- ¹⁹Eike Caldeweyher, Christoph Bannwarth, and Stefan Grimme. Extension of the D3 dispersion coefficient model. *J. Chem. Phys.*, 147(3):034112, 2017.
- ²⁰Marcus Elstner, Pavel Hobza, Thomas Frauenheim, Sándor Suhai, and Efthimios Kaxiras. Hydrogen bonding and stacking interactions of nucleic acid base pairs: A density-functional-theory based treatment. *J. Chem. Phys.*, 114(12):5149–5155, 2001.
- ²¹Stefan Grimme. Accurate description of van der Waals complexes by density functional theory including empirical corrections. *J. Comput. Chem.*, 25(12):1463–1473, 2004.
- ²²Stefan Grimme, Jens Antony, Stephan Ehrlich, and Helge Krieg. A consistent and accurate ab initio parametrization of density functional dispersion correction (DFT-D) for the 94 elements H-Pu. *J. Chem. Phys.*, 132(15):154104, 2010.
- ²³Petr Jurečka, Jiří Černý, Pavel Hobza, and Dennis R. Salahub. Density functional theory augmented with an empirical dispersion term. Interaction energies and geometries of 80 noncovalent complexes compared with ab initio quantum mechanics calculations. *J. Comput. Chem.*, 28(2):555–569, 2007.
- ²⁴Axel D. Becke and Erin R. Johnson. Exchange-hole dipole moment and the dispersion interaction. *J. Chem. Phys.*, 122(15):154104, 2005.
- ²⁵Axel D. Becke and Erin R. Johnson. A density-functional model of the dispersion interaction. *J. Chem. Phys.*, 123(15):154101, 2005.
- ²⁶Yasuhiro Iwabata and Hiromi Nakai. Local response dispersion method: A density-dependent dispersion correction for density functional theory. *Int. J. Quantum Chem.*, 115(5):309–324, 2015.
- ²⁷Takeshi Sato and Hiromi Nakai. Density functional method including weak interactions: Dispersion coefficients based on the local response approximation. *J. Chem. Phys.*, 131(22):224104, 2009.
- ²⁸Takeshi Sato and Hiromi Nakai. Local response dispersion method. II. Generalized multi-

- center interactions. *J. Chem. Phys.*, 133(19):194101, 2010.
- ²⁹B. M. Axilrod and E. Teller. Interaction of the van der Waals Type Between Three Atoms. *J. Chem. Phys.*, 11(6):299–300, 1943.
- ³⁰Yoshio Muto. Force between nonpolar molecules. *J. Phys. Math. Soc. Jpn*, 17:629–631, 1943.
- ³¹A. Otero-de-la-Roza, Luc M. LeBlanc, and Erin R. Johnson. Asymptotic Pairwise Dispersion Corrections Can Describe Layered Materials Accurately. *J. Phys. Chem. Lett.*, 11(6):2298–2302, 2020.
- ³²Erin R. Johnson. Chapter 5 - The Exchange-Hole Dipole Moment Dispersion Model. In Alberto Otero de la Roza and Gino A. DiLabio, editors, *Non-Covalent Interactions in Quantum Chemistry and Physics*, pages 169–194. Elsevier, January 2017.
- ³³A. Otero-de-la-Roza and Erin R. Johnson. Many-body dispersion interactions from the exchange-hole dipole moment model. *J. Chem. Phys.*, 138(5):054103, 2013.
- ³⁴Alberto Ambrosetti, Anthony M. Reilly, Robert A. DiStasio, and Alexandre Tkatchenko. Long-range correlation energy calculated from coupled atomic response functions. *J. Chem. Phys.*, 140(18):18A508, 2014.
- ³⁵Alexandre Tkatchenko, Robert A. DiStasio, Roberto Car, and Matthias Scheffler. Accurate and Efficient Method for Many-Body van der Waals Interactions. *Phys. Rev. Lett.*, 108(23):236402, 2012.
- ³⁶Alexandre Tkatchenko, Alberto Ambrosetti, and Robert A. DiStasio. Interatomic methods for the dispersion energy derived from the adiabatic connection fluctuation-dissipation theorem. *J. Chem. Phys.*, 138(7):074106, 2013.
- ³⁷Alberto Ambrosetti, Nicola Ferri, Robert A. DiStasio, and Alexandre Tkatchenko. Wave-like charge density fluctuations and van der waals interactions at the nanoscale. *Science*, 351(6278):1171–1176, 2016.
- ³⁸Anthony Stone. *The Theory of Intermolecular Forces*. Oxford University Press, 01 2013.
- ³⁹John F. Dobson, Angela White, and Angel Rubio. Asymptotics of the Dispersion Interaction: Analytic Benchmarks for van der Waals Energy Functionals. *Phys. Rev. Lett.*, 96(7):073201, 2006.
- ⁴⁰John F. Dobson. Towards efficient description of type-C London dispersion forces between low-dimensional metallic nanostructures. *Electron. Struct.*, 3(4):044001, 2021.

- ⁴¹K. Jackson, M. Yang, and J. Jellinek. Site-Specific Analysis of Dielectric Properties of Finite Systems. *J. Phys. Chem. C*, 111(48):17952–17960, 2007.
- ⁴²Koblar Jackson and Julius Jellinek. Si clusters are more metallic than bulk Si. *J. Chem. Phys.*, 145(24):244302, 2016.
- ⁴³John F. Dobson and Tim Gould. Calculation of dispersion energies. *J. Phys.: Condens. Matter*, 24(7):073201, 2012.
- ⁴⁴Nick Sablon, Frank De Proft, Paul W. Ayers, and Paul Geerlings. Computing Second-Order Functional Derivatives with Respect to the External Potential. *J. Chem. Theory Comput.*, 6(12):3671–3680, 2010.
- ⁴⁵Alston J. Misquitta, James Spencer, Anthony J. Stone, and Ali Alavi. Dispersion interactions between semiconducting wires. *Phys. Rev. B*, 82(7):075312, 2010.
- ⁴⁶Alston J. Misquitta, Ryo Maezono, Neil D. Drummond, Anthony J. Stone, and Richard J. Needs. Anomalous nonadditive dispersion interactions in systems of three one-dimensional wires. *Phys. Rev. B*, 89(4):045140, 2014.
- ⁴⁷Jianmin Tao, John P. Perdew, and Adrienn Ruzsinszky. Accurate van der Waals coefficients from density functional theory. *Proc. Natl. Acad. Sci.*, 109(1):18–21, 2012.
- ⁴⁸Adrienn Ruzsinszky, John P. Perdew, Jianmin Tao, Gábor I. Csonka, and J. M. Pitarke. Van der Waals Coefficients for Nanostructures: Fullerenes Defy Conventional Wisdom. *Phys. Rev. Lett.*, 109(23):233203, 2012.
- ⁴⁹A. Krishtal, P. Senet, M. Yang, and C. Van Alsenoy. A Hirshfeld partitioning of polarizabilities of water clusters. *J. Chem. Phys.*, 125(3):034312, 2006.
- ⁵⁰Brad A. Bauer, Timothy R. Lucas, Alisa Krishtal, Christian Van Alsenoy, and Sandeep Patel. Variation of Ion Polarizability from Vacuum to Hydration: Insights from Hirshfeld Partitioning. *J. Phys. Chem. A*, 114(34):8984–8992, 2010.
- ⁵¹Alisa Krishtal, Patrick Senet, and Christian Van Alsenoy. Influence of Structure on the Polarizability of Hydrated Methane Sulfonic Acid Clusters. *J. Chem. Theory Comput.*, 4(12):2122–2129, 2008.
- ⁵²Alisa Krishtal, Patrick Senet, and Christian Van Alsenoy. Origin of the size-dependence of the polarizability per atom in heterogeneous clusters: The case of AIP clusters. *J. Chem. Phys.*, 133(15):154310, 2010.
- ⁵³Ye Mei, Andrew C. Simmonett, Frank C. IV Pickard, Robert A. Jr. DiStasio, Bernard R.

- Brooks, and Yihan Shao. Numerical Study on the Partitioning of the Molecular Polarizability into Fluctuating Charge and Induced Atomic Dipole Contributions. *J. Phys. Chem. A*, 119(22):5865–5882, 2015.
- ⁵⁴Mario Galante and Alexandre Tkatchenko. Anisotropic van der waals dispersion forces in polymers: Structural symmetry breaking leads to enhanced conformational search. *Phys. Rev. Res.*, 5:L012028, 2023.
- ⁵⁵A. J. Stone. Distributed multipole analysis, or how to describe a molecular charge distribution. *Chem. Phys. Lett.*, 83(2):233–239, 1981.
- ⁵⁶Laura Gagliardi, Roland Lindh, and Gunnar Karlström. Local properties of quantum chemical systems: The LoProp approach. *J. Chem. Phys.*, 121(10):4494–4500, 2004.
- ⁵⁷Ignat Harczuk, Balazs Nagy, Frank Jensen, Olav Vahtras, and Hans Ågren. Local decomposition of imaginary polarizabilities and dispersion coefficients. *Phys. Chem. Chem. Phys.*, 19(30):20241–20250, 2017.
- ⁵⁸Dennis Elking, Tom Darden, and Robert J. Woods. Gaussian induced dipole polarization model. *J. Comput. Chem.*, 28(7):1261–1274, 2007.
- ⁵⁹W. C. Lu, C. Z. Wang, M. W. Schmidt, L. Bytautas, K. M. Ho, and K. Ruedenberg. Molecule intrinsic minimal basis sets. I. Exact resolution of ab initio optimized molecular orbitals in terms of deformed atomic minimal-basis orbitals. *J. Chem. Phys.*, 120(6):2629–2637, 2004.
- ⁶⁰Gerald Knizia. Intrinsic Atomic Orbitals: An Unbiased Bridge between Quantum Theory and Chemical Concepts. *J. Chem. Theory Comput.*, 9(11):4834–4843, 2013.
- ⁶¹Aaron C. West, Michael W. Schmidt, Mark S. Gordon, and Klaus Ruedenberg. A comprehensive analysis of molecule-intrinsic quasi-atomic, bonding, and correlating orbitals. I. Hartree-Fock wave functions. *J. Chem. Phys.*, 139(23):234107, 2013.
- ⁶²Tomasz Janowski. Near Equivalence of Intrinsic Atomic Orbitals and Quasiatomic Orbitals. *J. Chem. Theory Comput.*, 10(8):3085–3091, 2014.
- ⁶³Alston J. Misquitta and Anthony J. Stone. Distributed polarizabilities obtained using a constrained density-fitting algorithm. *J. Chem. Phys.*, 124(2):024111, 2006.
- ⁶⁴Keith E. Laidig and Richard F. W. Bader. Properties of atoms in molecules: Atomic polarizabilities. *J. Chem. Phys.*, 93(10):7213–7224, 1990.
- ⁶⁵P.L.A. Popelier. *Atoms in Molecules: An Introduction*. Prentice Hall, 2000.

- ⁶⁶F. L. Hirshfeld. Bonded-atom fragments for describing molecular charge densities. *Theoret. Chim. Acta*, 44(2):129–138, 1977.
- ⁶⁷Patrick Bultinck, Christian Van Alsenoy, Paul W. Ayers, and Ramon Carbó-Dorca. Critical analysis and extension of the Hirshfeld atoms in molecules. *J. Chem. Phys.*, 126(14):144111, 2007.
- ⁶⁸T. C. Lillestolen and R. J. Wheatley. First-Principles Calculation of Local Atomic Polarizabilities. *J. Phys. Chem. A*, 111(43):11141–11146, 2007.
- ⁶⁹Alston J. Misquitta and Anthony J. Stone. ISA-pol: distributed polarizabilities and dispersion models from a basis-space implementation of the iterated stockholder atoms procedure. *Theor. Chem. Acc.*, 137(11):153, 2018.
- ⁷⁰T. Verstraelen, P. W. Ayers, V. Van Speybroeck, and M. Waroquier. ACKS2: Atom-condensed Kohn-Sham DFT approximated to second order. *J. Chem. Phys.*, 138(7):074108, 2013.
- ⁷¹Toon Verstraelen, Steven Vandenbrande, and Paul W. Ayers. Direct computation of parameters for accurate polarizable force fields. *J. Chem. Phys.*, 141(19):194114, 2014.
- ⁷²YingXing Cheng and Toon Verstraelen. A new framework for frequency-dependent polarizable force fields. *J. Chem. Phys.*, 157(12):124106, 2022.
- ⁷³Toon Verstraelen, Steven Vandenbrande, Farnaz Heidar-Zadeh, Louis Vanduyfhuys, Veronique Van Speybroeck, Michel Waroquier, and Paul W. Ayers. Minimal basis iterative stockholder: Atoms in molecules for force-field development. *J. Chem. Theory Comput.*, 12(8):3894–3912, 2016.
- ⁷⁴A.J. Stone. Distributed polarizabilities. *Mol. Phys.*, 56(5):1065–1082, 1985.
- ⁷⁵Alston J. Misquitta and Anthony J. Stone. Dispersion energies for small organic molecules: First row atoms. *Mol. Phys.*, 106(12-13):1631–1643, 2008.
- ⁷⁶Nicolás Otero, Christian Van Alsenoy, Claude Pouchan, and Panagiotis Karamanis. Hirshfeld-based intrinsic polarizability density representations as a tool to analyze molecular polarizability. *J. Comput. Chem.*, 36(24):1831–1843, 2015.
- ⁷⁷András Olasz, Kenno Vanommeslaeghe, Alisa Krishtal, Tamás Veszprémi, Christian Van Alsenoy, and Paul Geerlings. The use of atomic intrinsic polarizabilities in the evaluation of the dispersion energy. *J. Chem. Phys.*, 127(22):224105, 2007.
- ⁷⁸Alisa Krishtal, Patrick Senet, and Christian Van Alsenoy. Local softness, softness dipole,

- and polarizabilities of functional groups: Application to the side chains of the 20 amino acids. *J. Chem. Phys.*, 131(4):044312, 2009.
- ⁷⁹D. Geldof, A. Krishtal, P. Geerlings, and C. Van Alsenoy. Partitioning of Higher Multipole Polarizabilities: Numerical Evaluation of Transferability. *J. Phys. Chem. A*, 115(45):13096–13103, 2011.
- ⁸⁰Greg J. Williams and Anthony J. Stone. Distributed dispersion: A new approach. *J. Chem. Phys.*, 119(9):4620–4628, 2003.
- ⁸¹N. El-Bakali Kassimi and Zijing Lin. Aza-Substituted Thiophene Derivatives: Structures, Dipole Moments, and Polarizabilities. *J. Phys. Chem. A*, 102(48):9906–9911, 1998.
- ⁸²Jean-François Truchon, Anthony Nicholls, Radu I. Iftimie, Benoît Roux, and Christopher I. Bayly. Accurate Molecular Polarizabilities Based on Continuum Electrostatics. *J. Chem. Theory Comput.*, 4(9):1480–1493, 2008.
- ⁸³A. J. Stone and R. J. A. Tough. Spherical tensor theory of long-range intermolecular forces. *Chem. Phys. Lett.*, 110(2):123–129, 1984.
- ⁸⁴W. Kohn and L. J. Sham. Self-consistent equations including exchange and correlation effects. *Phys. Rev.*, 140(4A):A1133–A1138, 1965.
- ⁸⁵Rick A. Kendall, Thom H. Dunning, and Robert J. Harrison. Electron affinities of the first-row atoms revisited. systematic basis sets and wave functions. *J. Chem. Phys.*, 96(9):6796–6806, 1992.
- ⁸⁶Toon Verstraelen, Pawel Tecmer, Farnaz Heidar-Zadeh, Cristina E. González-Espinoza, Matthew Chan, Taewon D. Kim, Katharina Boguslawski, Stijn Fias, Steven Vandenbrande, Diego Berrocal, and Paul W. Ayers. Horton 2.1.1, 2017. Accessed on Jun 7, 2023.
- ⁸⁷Kestutis Aidas, Celestino Angeli, Keld L. Bak, Vebjørn Bakken, Radovan Bast, Linus Boman, Ove Christiansen, Renzo Cimiraglia, Sonia Coriani, Pål Dahle, Erik K. Dalskov, Ulf Ekström, Thomas Enevoldsen, Janus J. Eriksen, Patrick Ettenhuber, Berta Fernández, Lara Ferrighi, Heike Fliegl, Luca Frediani, Kasper Hald, Asger Halkier, Christof Hättig, Hanne Heiberg, Trygve Helgaker, Alf Christian Hennum, Hinne Hettema, Eirik Hjertenaes, Stinne Høst, Ida-Marie Høyvik, Maria Francesca Iozzi, Branislav Jansík, Hans Jørgen Aa. Jensen, Dan Jonsson, Poul Jørgensen, Joanna Kauczor, Sheela Kirpekar, Thomas Kjaergaard, Wim Klopper, Stefan Knecht, Rika Kobayashi, Henrik Koch, Jacob Kongsted, Andreas Krapp, Kasper Kristensen, Andrea Ligabue, Ola B. Lutnaes, Juan I. Melo,

Kurt V. Mikkelsen, Rolf H. Myhre, Christian Neiss, Christian B. Nielsen, Patrick Norman, Jeppe Olsen, Jógvan Magnus H. Olsen, Anders Osted, Martin J. Packer, Filip Pawłowski, Thomas B. Pedersen, Patricio F. Provasi, Simen Reine, Zilvinas Rinkevicius, Torgeir A. Ruden, Kenneth Ruud, Vladimir V. Rybkin, Pawel Sałek, Claire C. M. Samson, Alfredo Sánchez de Merás, Trond Saue, Stephan P. A. Sauer, Bernd Schimmelpfennig, Kristian Sneskov, Arnfinn H. Steindal, Kristian O. Sylvester-Hvid, Peter R. Taylor, Andrew M. Teale, Erik I. Tellgren, David P. Tew, Andreas J. Thorvaldsen, Lea Thøgersen, Olav Vahtras, Mark A. Watson, David J. D. Wilson, Marcin Ziolkowski, and Hans Ågren. The dalton quantum chemistry program system. *Wiley Interdiscip. Rev.: Comput. Mol. Sci.*, 4(3):269–284, 2013.

⁸⁸Marc Montilla, Josep M. Luis, and Pedro Salvador. Origin-independent decomposition of the static polarizability. *J. Chem. Theory Comput.*, 17(2):1098–1105, 2021.

⁸⁹B.T. Thole. Molecular polarizabilities calculated with a modified dipole interaction. *Chem. Phys.*, 59(3):341–350, 1981.

⁹⁰Guillaume Lamoureux, Alexander D. MacKerell, and Benoît Roux. A simple polarizable model of water based on classical drude oscillators. *J. Chem. Phys.*, 119(10):5185–5197, 2003.

⁹¹Pengyu Ren, Chuanjie Wu, and Jay W. Ponder. Polarizable atomic multipole-based molecular mechanics for organic molecules. *J. Chem. Theory Comput.*, 7(10):3143–3161, 2011.

⁹²Qinghui Ge, Yuezhi Mao, and Martin Head-Gordon. Energy decomposition analysis for exciplexes using absolutely localized molecular orbitals. *J. Chem. Phys.*, 148(6):064105, 2018.

⁹³Francesco Ferdinando Summa, Guglielmo Monaco, Paolo Lazzeretti, and Riccardo Zanasi. Origin-independent densities of static and dynamic molecular polarizabilities. *J. Phys. Chem. Lett.*, 12(36):8855–8864, 2021.